



**The Abdus Salam
International Centre for Theoretical Physics**



2328-6

**Preparatory School to the Winter College on Optics and the Winter College on
Optics: Advances in Nano-Optics and Plasmonics**

6 - 17 February, 2012

**Direct Space Integral Equation Method for Numerical Investigation of Linear
and Nonlinear Optical Properties of Arbitrary Shaped Nanostructures**

M. Centini
SAPIENZA Università' di Roma
Roma
Italy



The Abdus Salam
International Centre for Theoretical Physics



**Winter College on Optics:
Advances in Nano-Optics and Plasmonics**
(6-17 February 2012)

**Direct Space Integral Equation Method for Numerical Investigation of
Linear and Nonlinear Optical Properties of
Arbitrary Shaped Nanostructures**

M.Centini

SAPIENZA Universita' di Roma, Roma, Italy

OUTLINE

- 1) Theoretical approach – description of the integration method;
- 2) Second harmonic generation in noncentrosymmetric nanocrystals;
- 3) Second harmonic generation in metal nanoparticles: Surface and bulk contributions;
- 4) EXAMPLES:
 - Second Harmonic Generation in Gold Nanoantennas, Bulk and surface contributions by far field pattern analysis;
 - Second harmonic generation by Excitation of Coupled Two Dimensional Silver Nanoresonators.
- 5) CONCLUSIONS

We consider a material system of arbitrary shape embedded in a homogeneous, non magnetic, dielectric medium with relative permittivity ϵ_b .

Properties of the object are described by an effective current density \underline{J} and charge density ρ .

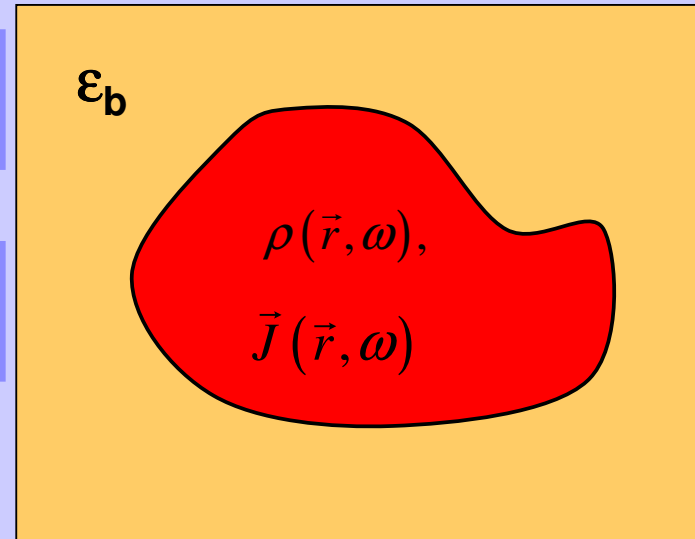
The ω -Fourier transforms of the four Maxwell equations are:

$$\epsilon_0 \epsilon_b(\omega) \nabla \cdot \vec{E}(\vec{r}, \omega) = \rho(\vec{r}, \omega), \quad (1)$$

$$\nabla \cdot \vec{B}(\vec{r}, \omega) = 0, \quad (2)$$

$$\nabla \times \vec{E}(\vec{r}, \omega) = i\omega \epsilon_0 \vec{H}(\vec{r}, \omega), \quad (3)$$

$$\nabla \times \vec{H}(\vec{r}, \omega) = -i\omega \epsilon_0 \epsilon_b(\omega) \vec{E}(\vec{r}, \omega) + \vec{J}(\vec{r}, \omega), \quad (4)$$



$$\text{with: } \vec{D} = \epsilon_0 \hat{\epsilon}_b \vec{E}, \quad \vec{B} = \epsilon_0 \vec{H}.$$

For the electric field, we can proceed as follows: from eq. (3) we have

$$\nabla \times \nabla \times \vec{E}(\vec{r}, \omega) = i\omega \epsilon_0 \nabla \times \vec{H}(\vec{r}, \omega),$$

And substituting eq. (4) we obtain:

$$\nabla \times \nabla \times \vec{E}(\vec{r}, \omega) = i\omega \epsilon_0 \left[-i\omega \epsilon_0 \epsilon_b(\omega) \vec{E}(\vec{r}, \omega) + \vec{J}(\vec{r}, \omega) \right], \quad (5)$$

We then apply the identity:

$$\vec{\nabla} \times \vec{\nabla} \times \vec{E}(\vec{r}, \omega) = \vec{\nabla}(\vec{\nabla} \cdot \vec{E}(\vec{r}, \omega)) - \nabla^2 \vec{E}(\vec{r}, \omega),$$

And eq. (5) becomes:

$$\vec{\nabla}(\vec{\nabla} \cdot \vec{E}(\vec{r}, \omega)) - \nabla^2 \vec{E}(\vec{r}, \omega) = i\omega \epsilon_0 \left[-i\omega \epsilon_0 \epsilon_b(\omega) \vec{E}(\vec{r}, \omega) + \vec{J}(\vec{r}, \omega) \right], \quad (6)$$

Finally we introduce the following relationship between charge, current and polarization densities:

$$\begin{aligned}\rho(\vec{r}, \omega) &= -\vec{\nabla} \cdot \vec{P}(\vec{r}, \omega), \\ \vec{J}(\vec{r}, \omega) &= -i\omega\vec{P}(\vec{r}, \omega),\end{aligned}$$

And equation (6) becomes:

$$\nabla^2 \vec{E}(\vec{r}, \omega) + \frac{\omega^2}{c^2} \epsilon_b(\omega) \vec{E}(\vec{r}, \omega) = -\omega^2 \epsilon_0 \vec{P}(\vec{r}, \omega) - \vec{\nabla} \left(\frac{\vec{\nabla} \cdot \vec{P}(\vec{r}, \omega)}{\epsilon_0 \epsilon_b(\omega)} \right),$$

which can be written as:

$$\left[\nabla^2 + \frac{\omega^2}{c^2} \epsilon_b(\omega) \right] \vec{E}(\vec{r}, \omega) = -\frac{1}{\epsilon_0} \left[\frac{\omega^2}{c^2} + \frac{\vec{\nabla} \vec{\nabla}}{\epsilon_b(\omega)} \right] \cdot \vec{P}(\vec{r}, \omega), \quad (7)$$

If we define the following operators:

$$\widehat{O} = \left[\nabla^2 + k_0^2 \epsilon_b(\omega) \right];$$
$$\widehat{Q} = \left[k_0^2 + \frac{1}{\epsilon_b(\omega)} \vec{\nabla} \vec{\nabla} \right];$$

with $k_0 = \omega/c$

The equation (7) can be rewritten as:

$$\widehat{O} \vec{E}(\vec{r}, \omega) = -\frac{1}{\epsilon_0} \widehat{Q} \vec{P}(\vec{r}, \omega), \quad (8)$$

we can express the particular solution of (8) as follows:

$$\vec{E}(\vec{r}, \omega) = -\frac{1}{\epsilon_0} \widehat{O}^{-1} \widehat{Q} \cdot \vec{P}(\vec{r}, \omega) = -\frac{1}{\epsilon_0} \widehat{O}^{-1} \int \widehat{Q} \cdot \vec{P}(\vec{r}', \omega) \delta(\vec{r} - \vec{r}') d\vec{r}',$$

Operator \hat{O}^{-1} can be moved inside the integral if the integrand is not singular:

$$\vec{E}(\vec{r}, \omega) = -\frac{1}{\epsilon_0} \int \hat{O}^{-1} \hat{Q} \cdot \vec{P}(\vec{r}', \omega) \delta(\vec{r} - \vec{r}') d\vec{r}' = \frac{1}{\epsilon_0} \int \bar{\bar{S}}_0(\vec{r}, \vec{r}', \omega) \cdot \vec{P}(\vec{r}', \omega) d\vec{r}',$$

Where we defined the field-susceptibility tensor:

$$\bar{\bar{S}}_0(\vec{r}, \vec{r}', \omega) = -\hat{O}^{-1} \hat{Q} \delta(\vec{r} - \vec{r}'),$$

NOTE: Impossibility of interchanging the operators the integral equation when the integrand becomes singular, i.e. when $r \rightarrow r'$ *requires further analysis and it is responsible of an additional source term (it will be discussed later).*

The general solution is obtained by adding the solution of the homogeneous equation i.e. the field in the absence of the nanostructure.

$$\vec{E}(\vec{r}, \omega) = \vec{E}_0(\vec{r}, \omega) + \frac{1}{\epsilon_0} \int \vec{S}_0(\vec{r}, \vec{r}', \omega) \cdot \vec{P}(\vec{r}', \omega) d\vec{r}',$$

Incident field

Scattered field

If the nanostructure can be described by a macroscopic dielectric susceptibility we can write:

$$\vec{P}(\vec{r}', \omega) = \epsilon_0 \chi_{0b}(\vec{r}', \omega) \vec{E}(\vec{r}', \omega),$$

Where χ_{0b} is the difference between the dielectric constant of the nanostructure and that of the surroundings:

$$\chi_{0b}(\vec{r}', \omega) = \epsilon_r(\vec{r}', \omega) - \epsilon_b$$

The formal solution is:

$$\vec{E}(\vec{r}, \omega) = \vec{E}_0(\vec{r}, \omega) + \int \bar{\bar{S}}_0(\vec{r}, \vec{r}', \omega) \cdot \chi_{ob}(\vec{r}', \omega) \vec{E}(\vec{r}', \omega) d\vec{r}', \quad (9)$$

The next step is to give an explicit expression for the S_0 operator:

$$\bar{\bar{S}}_0(\vec{r}, \vec{r}', \omega) = -\hat{O}^{-1} \hat{Q} \delta(\vec{r} - \vec{r}'),$$

For the operator O
it is known that:

$$\hat{O}G_{ob}(\vec{r}, \vec{r}', \omega) = [\nabla^2 + k_b^2]G_{ob}(\vec{r}, \vec{r}', \omega) = -\delta(\vec{r} - \vec{r}');$$

with $k_b^2 = k_0^2 \epsilon_b(\omega)$


Where G_0 is the scalar green function for the Helmholtz equation:

$$G_{ob}(\vec{r}, \vec{r}', \omega) = \frac{e^{ik_b|\vec{r}-\vec{r}'|}}{4\pi|\vec{r}-\vec{r}'|};$$

Thus:

$$G_{ob}(\vec{r}, \vec{r}', \omega) = -\hat{O}^{-1} \delta(\vec{r} - \vec{r}');$$

And finally:

$$\bar{\bar{S}}_0(\vec{r}, \vec{r}', \omega) = -\hat{O}^{-1} \hat{Q} \delta(\vec{r} - \vec{r}') = -\hat{Q} \hat{O}^{-1} \delta(\vec{r} - \vec{r}') = \hat{Q} G_{ob}(\vec{r}, \vec{r}', \omega),$$


Commutation between the operators is not possible if $r \rightarrow r'$. This operation is responsible for the appearance of an extra term and will be discussed later.

S_0 can be evaluated by calculating the following expression:

$$\bar{\bar{S}}_0(\vec{r}, \vec{r}', \omega) = \frac{k_0^2}{4\pi} \left[\bar{\bar{I}} + \frac{1}{k_b^2} \vec{\nabla} \vec{\nabla} \right] \frac{e^{ik_b |\vec{r} - \vec{r}'|}}{|\vec{r} - \vec{r}'|};$$

We define the Green dyadic for the electric field:

$$\begin{aligned} \bar{\bar{G}}_E(\vec{r}, \vec{r}', \omega) &= \frac{1}{4\pi} \left[\bar{\bar{I}} + \frac{1}{k_b^2} \vec{\nabla} \vec{\nabla} \right] \frac{e^{ik_b|\vec{r}-\vec{r}'|}}{|\vec{r}-\vec{r}'|} = \\ &= \left(\bar{\bar{I}} + \frac{ik_b R - 1}{k_b^2 R^2} \bar{\bar{I}} + \frac{3 - 3ik_b R - k_b^2 R^2}{k_b^2 R^4} \vec{R} \vec{R} \right) \frac{e^{ik_b R}}{4\pi R}; \end{aligned}$$

where $\vec{R} = \vec{r} - \vec{r}'$

We have:

$$\bar{\bar{S}}_0(\vec{r}, \vec{r}', \omega) = k_0^2 \bar{\bar{G}}_E(\vec{r}, \vec{r}', \omega);$$

In cartesian coordinates:

$$\begin{pmatrix} G_{xx} & G_{xy} & G_{xz} \\ G_{yx} & G_{yy} & G_{yz} \\ G_{zx} & G_{zy} & G_{zz} \end{pmatrix}$$

NOTE: The Green dyadic contains both far field (proportional to 1/R) and near field (proportional to 1/R² and 1/R³)

The equation for the electric field becomes:

$$\vec{E}(\vec{r}, \omega) = \vec{E}_0(\vec{r}, \omega) + \int_V k_0^2 \chi_{ob}(\vec{r}', \omega) \bar{\bar{G}}_E(\vec{r}, \vec{r}', \omega) \cdot \vec{E}(\vec{r}', \omega) d\vec{r}',$$

V is the volume of the nanostructure.

As mentioned before this expression is not valid for $r=r'$. A small volume V_δ containing r must be excluded. The commutation of operators O and Q generates an additional source dyadic term \mathbf{L} depending on the shape of the exclusion volume V_δ .

Its derivation is given with much detail by Yaghjian*.

For a spherical volume it can be shown that:

$$\bar{\bar{L}} = \frac{1}{3} \bar{\bar{I}},$$

*A. D. Yaghjian, Proc. of the IEEE, Vol. 68, No.2 248-63 (1980).

And the general expression for the equation is:

$$\vec{E}(\vec{r}, \omega) = \vec{E}_0(\vec{r}, \omega) + \lim_{V_\delta \rightarrow 0} \int_{V-V_\delta} k_0^2 \chi_{0b}(\vec{r}', \omega) \bar{\bar{G}}_E(\vec{r}, \vec{r}', \omega) \cdot \vec{E}(\vec{r}', \omega) d\vec{r}' - \bar{L} \frac{\chi_{0b}(\vec{r}, \omega)}{\epsilon_b(\omega)} \vec{E}(\vec{r}, \omega),$$

NOTE 1: When the observation point \mathbf{r} is located outside the scatterer, no singularity shows up since the integration is limited to the scatterer volume.

NOTE 2: the field at any point in the background is entirely determined from the field inside the scatterer.

This can be used to split the calculation: **in a first step** only the field inside the scatterer is computed and stored;

Second step: the field at any desired location in the background is then computed.

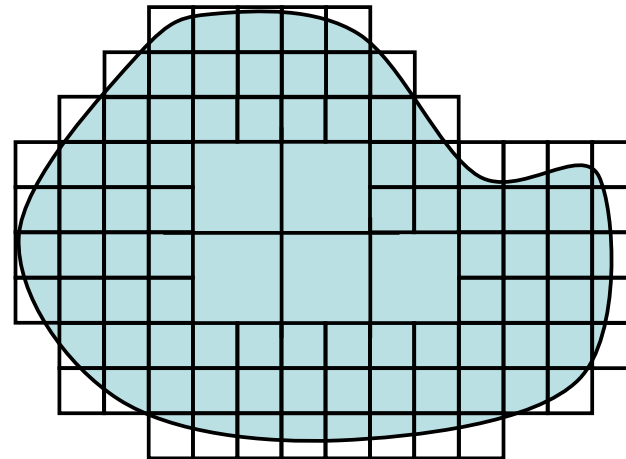
searching for exact solutions requires a volume discretization procedure of the source region*

We define a grid with N meshes over the system.

Each mesh i is centered at position \mathbf{r}_i and has a volume V_i .

Different size meshes can be combined

higher mesh refinement can be used where a precise knowledge of the field is required or where the dielectric contrast with respect to the background is large (i.e. $\chi_{ob} \gg 1$)



*O.J.F. Martin and N.B. Piller, Phys. Rev. E, Vol 58, 3 (1998)

Introducing:

the discretized field
the discretized dielectric susceptibility
the discretized Green's tensor

$$\mathbf{E}_i = \mathbf{E}(\mathbf{r}_i),$$
$$\chi_{b,i} = \chi_{ob}(\mathbf{r}_i)$$

$$\bar{\bar{G}}_E(\vec{r}, \vec{r}', \omega) = G_{i,j}$$

we obtain a dense system of linear equations:

$$\vec{E}_i = \vec{E}_{0,i} + \sum_{j=1, j \neq i}^N \bar{\bar{G}}_{i,j} \cdot [k_0^2 \chi_{b,j} \vec{E}_j] \Delta \tau_j$$
$$+ \bar{M}_i \cdot k_0^2 \chi_{b,i} \vec{E}_i - \bar{L} \frac{\chi_{b,i}}{\epsilon_b} \vec{E}_i;$$

$$\vec{E}(\vec{r}, \omega) = \vec{E}_0(\vec{r}, \omega) + \lim_{V_\delta \rightarrow 0} \int_{V-V_\delta} k_0^2 \chi_{ob}(\vec{r}', \omega) \bar{\bar{G}}_E(\vec{r}, \vec{r}', \omega) \cdot \vec{E}(\vec{r}', \omega) d\vec{r}' - \bar{L} \frac{\chi_{ob}(\vec{r}, \omega)}{\epsilon_b(\omega)} \vec{E}(\vec{r}, \omega),$$

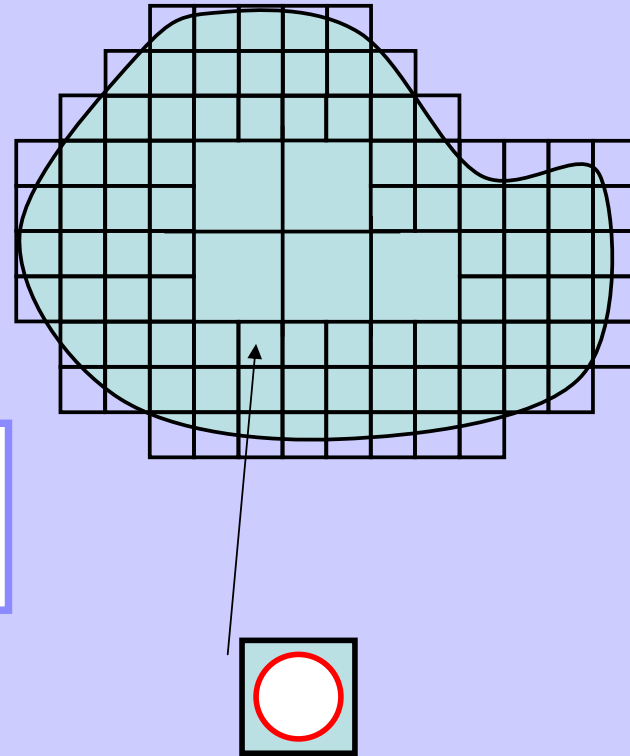
Where:

$$\bar{\bar{M}}_i = \lim_{V_\delta \rightarrow 0} \int_{\Delta\tau_i - V_\delta} \bar{\bar{G}}_E(\vec{r}_i, \vec{r}') d\vec{r}';$$

The value of M_i can be evaluated analytically for a mesh with a simple shape (i.e. cubic or spherical). For a spherical mesh we have:

$$\bar{\bar{M}}_i = \frac{2}{3k_b^2} \left[(1 - ik_b R_i^{eff}) e^{ik_b R_i^{eff}} - 1 \right] \bar{\bar{I}},$$

$$R_i^{eff} = \left(\frac{3}{4\pi} \Delta\tau_i \right)^{\frac{1}{3}};$$



* O.J.F. Martin and N.B. Piller, Phys. Rev. E, Vol 58, 3 (1998)

Numerical implementation of the algorithm

Starting with the discretized equation:

$$\begin{aligned}\vec{E}_i = \vec{E}_{0,i} + \sum_{j=1, j \neq i}^N \overline{\overline{G}}_{i,j} \cdot \left[k_0^2 \chi_{b,j} \vec{E}_j \right] \Delta \tau_j \\ + \overline{\overline{M}}_i \cdot k_0^2 \chi_{b,i} \vec{E}_i - \overline{\overline{L}} \frac{\chi_{b,i}}{\epsilon_b} \vec{E}_i;\end{aligned}$$

We define the array containing the input field E_0 as:

$$\overline{\overline{B}} = \left(E_{0,1}^x \quad E_{0,2}^x \quad \dots \quad E_{0,N}^x \quad E_{0,1}^y \quad E_{0,2}^y \quad \dots \quad E_{0,N}^y \quad E_{0,1}^z \quad E_{0,2}^z \quad \dots \quad E_{0,N}^z \right);$$

The same procedure is performed for the total field:

$$\overline{\overline{X}} = \left(E_1^x \quad E_2^x \quad \dots \quad E_N^x \quad E_1^y \quad E_2^y \quad \dots \quad E_N^y \quad E_1^z \quad E_2^z \quad \dots \quad E_N^z \right);$$

B and X are an arrays composed by 3N elements

Numerical implementation of the algorithm

$$\begin{bmatrix}
 \begin{pmatrix} 0 & G_{1,2}^{xx} & \dots & G_{1,N}^{xx} \\ G_{2,1}^{xx} & 0 & \dots & G_{2,N}^{xx} \\ \dots & \dots & \dots & \dots \\ G_{N,1}^{xx} & G_{N,2}^{xx} & \dots & 0 \end{pmatrix} &
 \begin{pmatrix} 0 & G_{1,2}^{xy} & \dots & G_{1,N}^{xy} \\ G_{2,1}^{xy} & 0 & \dots & G_{2,N}^{xy} \\ \dots & \dots & \dots & \dots \\ G_{N,1}^{xy} & G_{N,2}^{xy} & \dots & 0 \end{pmatrix} &
 \begin{pmatrix} 0 & G_{1,2}^{xz} & \dots & G_{1,N}^{xz} \\ G_{2,1}^{xz} & 0 & \dots & G_{2,N}^{xz} \\ \dots & \dots & \dots & \dots \\ G_{N,1}^{xz} & G_{N,2}^{xz} & \dots & 0 \end{pmatrix} \\
 \begin{pmatrix} 0 & G_{1,2}^{yx} & \dots & G_{1,N}^{yx} \\ G_{2,1}^{yx} & 0 & \dots & G_{2,N}^{yx} \\ \dots & \dots & \dots & \dots \\ G_{N,1}^{yx} & G_{N,2}^{yx} & \dots & 0 \end{pmatrix} &
 \begin{pmatrix} 0 & G_{1,2}^{yy} & \dots & G_{1,N}^{yy} \\ G_{2,1}^{yy} & 0 & \dots & G_{2,N}^{yy} \\ \dots & \dots & \dots & \dots \\ G_{N,1}^{yy} & G_{N,2}^{yy} & \dots & 0 \end{pmatrix} &
 \begin{pmatrix} 0 & G_{1,2}^{yz} & \dots & G_{1,N}^{yz} \\ G_{2,1}^{yz} & 0 & \dots & G_{2,N}^{yz} \\ \dots & \dots & \dots & \dots \\ G_{N,1}^{yz} & G_{N,2}^{yz} & \dots & 0 \end{pmatrix} \\
 \begin{pmatrix} 0 & G_{1,2}^{zx} & \dots & G_{1,N}^{zx} \\ G_{2,1}^{zx} & 0 & \dots & G_{2,N}^{zx} \\ \dots & \dots & \dots & \dots \\ G_{N,1}^{zx} & G_{N,2}^{zx} & \dots & 0 \end{pmatrix} &
 \begin{pmatrix} 0 & G_{1,2}^{zy} & \dots & G_{1,N}^{zy} \\ G_{2,1}^{zy} & 0 & \dots & G_{2,N}^{zy} \\ \dots & \dots & \dots & \dots \\ G_{N,1}^{zy} & G_{N,2}^{zy} & \dots & 0 \end{pmatrix} &
 \begin{pmatrix} 0 & G_{1,2}^{zz} & \dots & G_{1,N}^{zz} \\ G_{2,1}^{zz} & 0 & \dots & G_{2,N}^{zz} \\ \dots & \dots & \dots & \dots \\ G_{N,1}^{zz} & G_{N,2}^{zz} & \dots & 0 \end{pmatrix}
 \end{bmatrix}$$

Discretized G tensor is numerically composed by a 3Nx3N matrix. The zeroes take into account the fact that the sum is performed over the indices i,j excluding the i=j terms

Numerical implementation of the algorithm

$$\sum_{j=1, j \neq i}^N \bar{G}_{i,j} \cdot \left[k_0^2 \chi_{b,j} \vec{E}_j \right] \Delta \tau_j$$

$$k_0^2 \begin{pmatrix} \begin{pmatrix} 0 & \chi_2 \Delta \tau_2 G_{1,2}^{xx} & \dots & \chi_N \Delta \tau_N G_{1,N}^{xx} \\ \chi_1 \Delta \tau_1 G_{2,1}^{xx} & 0 & \dots & \chi_N \Delta \tau_N G_{2,N}^{xx} \\ \dots & \dots & \dots & \dots \\ \chi_1 \Delta \tau_1 G_{N,1}^{xx} & \chi_2 \Delta \tau_2 G_{N,2}^{xx} & \dots & 0 \end{pmatrix} & \begin{pmatrix} 0 & \chi_2 \Delta \tau_2 G_{1,2}^{xy} & \dots & \chi_N \Delta \tau_N G_{1,N}^{xy} \\ \chi_1 \Delta \tau_1 G_{2,1}^{xy} & 0 & \dots & \chi_N \Delta \tau_N G_{2,N}^{xy} \\ \dots & \dots & \dots & \dots \\ \chi_1 \Delta \tau_1 G_{N,1}^{xy} & \chi_2 \Delta \tau_2 G_{N,2}^{xy} & \dots & 0 \end{pmatrix} & \begin{pmatrix} 0 & \chi_2 \Delta \tau_2 G_{1,2}^{xz} & \dots & \chi_N \Delta \tau_N G_{1,N}^{xz} \\ \chi_1 \Delta \tau_1 G_{2,1}^{xz} & 0 & \dots & \chi_N \Delta \tau_N G_{2,N}^{xz} \\ \dots & \dots & \dots & \dots \\ \chi_1 \Delta \tau_1 G_{N,1}^{xz} & \chi_2 \Delta \tau_2 G_{N,2}^{xz} & \dots & 0 \end{pmatrix} \\ \begin{pmatrix} 0 & \chi_2 \Delta \tau_2 G_{1,2}^{yx} & \dots & \chi_N \Delta \tau_N G_{1,N}^{yx} \\ \chi_1 \Delta \tau_1 G_{2,1}^{yx} & 0 & \dots & \chi_N \Delta \tau_N G_{2,N}^{yx} \\ \dots & \dots & \dots & \dots \\ \chi_1 \Delta \tau_1 G_{N,1}^{yx} & \chi_2 \Delta \tau_2 G_{N,2}^{yx} & \dots & 0 \end{pmatrix} & \begin{pmatrix} 0 & \chi_2 \Delta \tau_2 G_{1,2}^{yy} & \dots & \chi_N \Delta \tau_N G_{1,N}^{yy} \\ \chi_1 \Delta \tau_1 G_{2,1}^{yy} & 0 & \dots & \chi_N \Delta \tau_N G_{2,N}^{yy} \\ \dots & \dots & \dots & \dots \\ \chi_1 \Delta \tau_1 G_{N,1}^{yy} & \chi_2 \Delta \tau_2 G_{N,2}^{yy} & \dots & 0 \end{pmatrix} & \begin{pmatrix} 0 & \chi_2 \Delta \tau_2 G_{1,2}^{yz} & \dots & \chi_N \Delta \tau_N G_{1,N}^{yz} \\ \chi_1 \Delta \tau_1 G_{2,1}^{yz} & 0 & \dots & \chi_N \Delta \tau_N G_{2,N}^{yz} \\ \dots & \dots & \dots & \dots \\ \chi_1 \Delta \tau_1 G_{N,1}^{yz} & \chi_2 \Delta \tau_2 G_{N,2}^{yz} & \dots & 0 \end{pmatrix} \\ \begin{pmatrix} 0 & \chi_2 \Delta \tau_2 G_{1,2}^{zx} & \dots & \chi_N \Delta \tau_N G_{1,N}^{zx} \\ \chi_1 \Delta \tau_1 G_{2,1}^{zx} & 0 & \dots & \chi_N \Delta \tau_N G_{2,N}^{zx} \\ \dots & \dots & \dots & \dots \\ \chi_1 \Delta \tau_1 G_{N,1}^{zx} & \chi_2 \Delta \tau_2 G_{N,2}^{zx} & \dots & 0 \end{pmatrix} & \begin{pmatrix} 0 & \chi_2 \Delta \tau_2 G_{1,2}^{zy} & \dots & \chi_N \Delta \tau_N G_{1,N}^{zy} \\ \chi_1 \Delta \tau_1 G_{2,1}^{zy} & 0 & \dots & \chi_N \Delta \tau_N G_{2,N}^{zy} \\ \dots & \dots & \dots & \dots \\ \chi_1 \Delta \tau_1 G_{N,1}^{zy} & \chi_2 \Delta \tau_2 G_{N,2}^{zy} & \dots & 0 \end{pmatrix} & \begin{pmatrix} 0 & \chi_2 \Delta \tau_2 G_{1,2}^{zz} & \dots & \chi_N \Delta \tau_N G_{1,N}^{zz} \\ \chi_1 \Delta \tau_1 G_{2,1}^{zz} & 0 & \dots & \chi_N \Delta \tau_N G_{2,N}^{zz} \\ \dots & \dots & \dots & \dots \\ \chi_1 \Delta \tau_1 G_{N,1}^{zz} & \chi_2 \Delta \tau_2 G_{N,2}^{zz} & \dots & 0 \end{pmatrix} \end{pmatrix} \begin{pmatrix} X_1 \\ X_2 \\ \dots \\ X_N \\ \dots \\ X_{2N} \\ \dots \\ X_{3N} \end{pmatrix}$$

Being:

$$= \bar{S} \cdot \bar{X}$$

$$\bar{X} = \left(E_1^x \quad E_2^x \quad \dots \quad E_N^x \quad E_1^y \quad E_2^y \quad \dots \quad E_N^y \quad E_1^z \quad E_2^z \quad \dots \quad E_N^z \right);$$

Numerical implementation of the algorithm

$$\overline{\overline{M}}_i \cdot k_0^2 \chi_{b,i} \vec{E}_i - \overline{\overline{L}} \frac{\chi_{b,i}}{\epsilon_b} \vec{E}_i;$$

$$\left\{ \begin{array}{l} A_i^{xx} = M_i^{xx} \cdot k_0^2 \chi_i - L^{xx} \frac{\chi_i}{\epsilon_b} \\ A_i^{yy} = M_i^{yy} \cdot k_0^2 \chi_i - L^{yy} \frac{\chi_i}{\epsilon_b} \\ A_i^{zz} = M_i^{zz} \cdot k_0^2 \chi_i - L^{zz} \frac{\chi_i}{\epsilon_b} \end{array} \right.$$

$$\left[\begin{array}{ccc} \begin{pmatrix} A_1^{xx} & 0 & \dots & 0 \\ 0 & A_2^{xx} & \dots & 0 \\ \dots & \dots & \dots & \dots \\ 0 & 0 & \dots & A_N^{xx} \end{pmatrix} & \begin{pmatrix} 0 & 0 & \dots & 0 \\ 0 & 0 & \dots & 0 \\ \dots & \dots & \dots & \dots \\ 0 & 0 & \dots & 0 \end{pmatrix} & \begin{pmatrix} 0 & 0 & \dots & 0 \\ 0 & 0 & \dots & 0 \\ \dots & \dots & \dots & \dots \\ 0 & 0 & \dots & 0 \end{pmatrix} \\ \begin{pmatrix} 0 & 0 & \dots & 0 \\ 0 & 0 & \dots & 0 \\ \dots & \dots & \dots & \dots \\ 0 & 0 & \dots & 0 \end{pmatrix} & \begin{pmatrix} A_1^{yy} & 0 & \dots & 0 \\ 0 & A_2^{yy} & \dots & 0 \\ \dots & \dots & \dots & \dots \\ 0 & 0 & \dots & A_N^{yy} \end{pmatrix} & \begin{pmatrix} 0 & 0 & \dots & 0 \\ 0 & 0 & \dots & 0 \\ \dots & \dots & \dots & \dots \\ 0 & 0 & \dots & 0 \end{pmatrix} \\ \begin{pmatrix} 0 & 0 & \dots & 0 \\ 0 & 0 & \dots & 0 \\ \dots & \dots & \dots & \dots \\ 0 & 0 & \dots & 0 \end{pmatrix} & \begin{pmatrix} 0 & 0 & \dots & 0 \\ 0 & 0 & \dots & 0 \\ \dots & \dots & \dots & \dots \\ 0 & 0 & \dots & 0 \end{pmatrix} & \begin{pmatrix} A_1^{zz} & 0 & \dots & 0 \\ 0 & A_2^{zz} & \dots & 0 \\ \dots & \dots & \dots & \dots \\ 0 & 0 & \dots & A_N^{zz} \end{pmatrix} \end{array} \right] \begin{pmatrix} X_1 \\ X_2 \\ \dots \\ X_N \\ \dots \\ X_{2N} \\ \dots \\ X_{3N} \end{pmatrix} = \overline{\overline{A}} \cdot \overline{\overline{X}}$$

Numerical implementation of the algorithm

Finally the equation can be written as:

$$\begin{aligned}\vec{E}_i = \vec{E}_{0,i} + \sum_{j=1, j \neq i}^N \bar{G}_{i,j} \cdot \left[k_0^2 \chi_{b,j} \vec{E}_j \right] \Delta \tau_j \\ + \bar{M}_i \cdot k_0^2 \chi_{b,i} \vec{E}_i - \bar{L} \frac{\chi_{b,i}}{\epsilon_b} \vec{E}_i;\end{aligned}$$

$$\bar{X} = (\bar{S} + \bar{A}) \cdot \bar{X} + \bar{B}$$

So, for a given array B describing the incident field in all the points of the scatterer, the total field can be evaluated by solving for the X variable the following system of equations:

$$\left(\bar{I} - \bar{S} - \bar{A} \right) \cdot \bar{X} = \bar{B} \quad \Longrightarrow \quad \bar{K} \cdot \bar{X} = \bar{B} \quad \Longrightarrow \quad \bar{X} = \bar{K}^{-1} \cdot \bar{B}$$

SUMMARY

- 1] Consider a nanostructure defined by a dielectric constant $\epsilon(r)$ embedded in a homogenous medium ϵ_b .
- 2] Define a grid with N meshes over the system. Each mesh i is centered at position \mathbf{r}_i and has a volume V_i .
- 3] Select an incident field (for example a plane wave) and calculate its value on the \mathbf{r}_i points ignoring the presence of the nanostructure. (constructing the \mathbf{B} array)
- 4] Calculate the $3N \times 3N$ \mathbf{K} -matrix by evaluating the Green tensor elements and the \mathbf{M} and \mathbf{L} operators for all the \mathbf{r}_i points.
- 5] Calculate \mathbf{K}^{-1} and evaluate the total field INSIDE THE SCATTERER by:

$$\bar{X} = \bar{K}^{-1} \cdot \bar{B}$$

STEP 2: Calculation of the field outside the scatterer

1B] Define the domain where you want to calculate the electric field. For example a plane at arbitrary distance from the object.

2B] Define a grid with M meshes over the selected domain.

The discretized equation is:

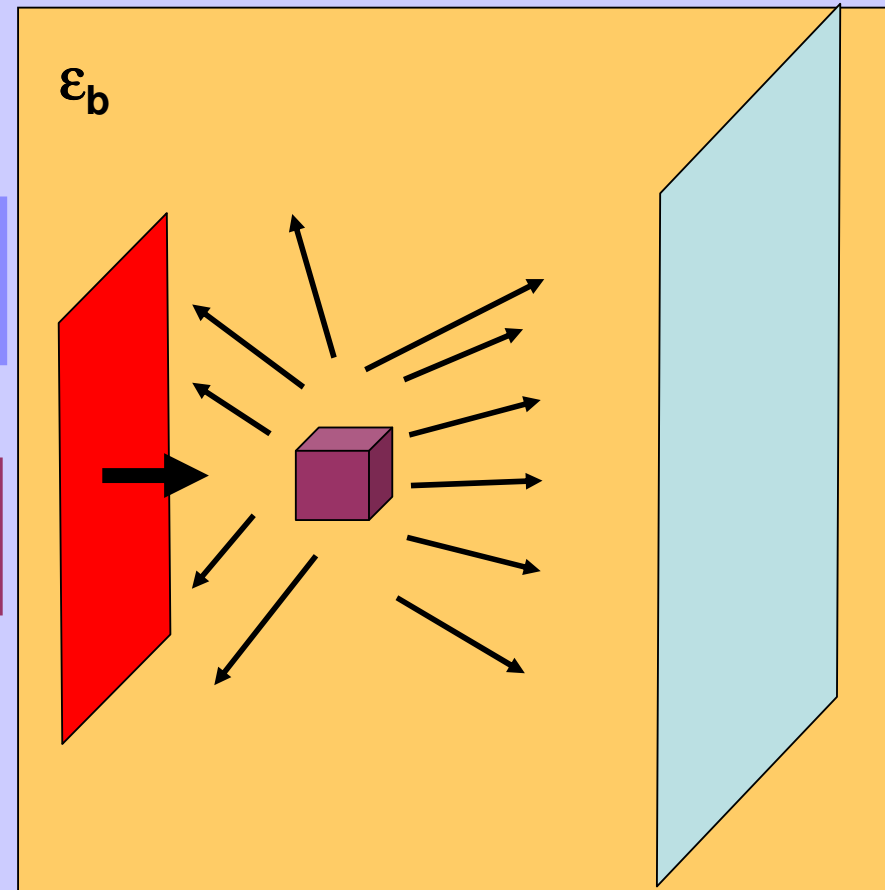
$$\vec{E}_{tot,i} = \vec{E}_{0,i} + \sum_{j=1, j \neq i}^N \overline{\overline{G}}_{i,j} [k_0^2 \chi_{b,j} \vec{E}_{P,j}] \Delta \tau_j$$

Incident field evaluated at the observation plane: $i=1, \dots, M$.

Field collected in the observation plane: $i=1, \dots, M$.

Field inside the scatterer calculated in step 1. $j=1, \dots, N$.

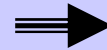
Link between the points of the objects and the points of the observation plane. Every components is a $M \times N$ matrix



STEP 2: Calculation of the field outside the scatterer

3B] Calculate the scattered field by evaluating:

$$\vec{E}_{sc,i} = \sum_{j=1, j \neq i}^N \bar{G}_{i,j} \cdot [k_0^2 \chi_{b,j} \vec{E}_{P,j}] \Delta \tau_j$$



$$\bar{Y} = \bar{S}_{ext} \bar{X};$$

3Mx3N

3N array
calculated in
step 1

4B] Calculate the total field by adding the incident field:

$$\vec{E}_{tot,i} = \vec{E}_{0,i} + \vec{E}_{sc,i}$$

NOTE: Step 2 can be repeated and the field outside the scatterer can be calculated everywhere in the space easier if the data from STEP 1 are saved. No matrix inversion is required for STEP 2, thus the process is faster.

Calculation of CROSS SECTIONS

In the absence of an obstacle, the average power carried across Σ by the incident wave is zero:

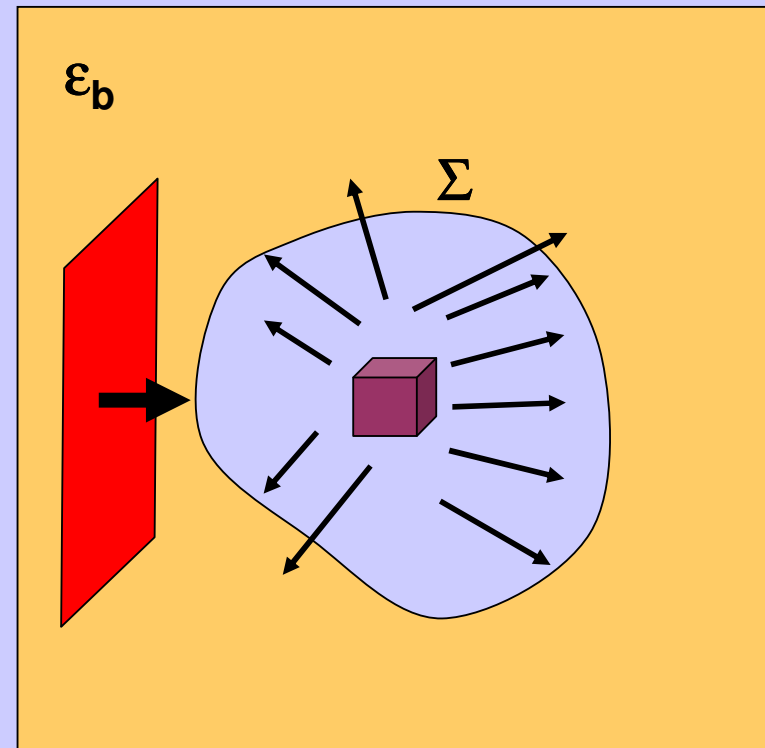
$$\frac{1}{2} \operatorname{Re} \int_{\Sigma} (\vec{E}_{tot} \times \vec{H}_{tot}^*) \cdot \hat{n} d\Sigma = \frac{1}{2} \operatorname{Re} \int_{\Sigma} (\vec{E}_{0,\omega} \times \vec{H}_{0,\omega}^*) \cdot \hat{n} d\Sigma = 0;$$

$$\vec{E}_{tot} = \vec{E}_0 + \vec{E}_{sc}$$

It means that no energy is extracted from the incident wave.

The presence of the obstacle is responsible for a scattered field and losses. If there is absorption the overall flux of the Poynting vector across Σ is negative i.e. the outgoing energy is less than the ingoing. **The absorbed power is:**

$$P_{abs} = -\frac{1}{2} \operatorname{Re} \int_{\Sigma} (\vec{E}_{tot} \times \vec{H}_{tot}^*) \cdot \hat{n} d\Sigma$$



Calculation of CROSS SECTIONS

The time-averaged power scattered by an obstacle is

$$P_{sc} = \frac{1}{2} \operatorname{Re} \int_{\Sigma} (\vec{E}_{sc} \times \vec{H}_{sc}^*) \cdot \hat{n} d\Sigma$$

NOTE: it is always a positive number

The total power **EXTRACTED** from the incident wave is:

$$P_{ext} = P_{abs} + P_{sc} = -\frac{1}{2} \operatorname{Re} \int_{\Sigma} (\vec{E}_{tot} \times \vec{H}_{tot}^* - \vec{E}_{sc} \times \vec{H}_{sc}^*) \cdot \hat{n} d\Sigma$$

$$\vec{E}_{tot} = \vec{E}_0 + \vec{E}_{sc}$$



$$P_{ext} = -\frac{1}{2} \operatorname{Re} \int_{\Sigma} (\vec{E}_0 \times \vec{H}_{sc}^* - \vec{E}_{sc} \times \vec{H}_0^*) \cdot \hat{n} d\Sigma$$

Calculation of CROSS SECTIONS

If the object is irradiated by a plane wave, the absorbed, scattered and extracted powers are proportional to the power density of the incident wave:

$$\mathcal{P}_0 = \frac{1}{2} \operatorname{Re} \left(\vec{E}_0 \times \vec{H}_0^* \right);$$

It is useful to define quantities that are related only to the object, size and material, called cross sections **[m²]** :

$$SCS = \frac{P_{sc}}{\mathcal{P}_0} = \frac{\operatorname{Re} \int_{\Sigma} \left(\vec{E}_{sc} \times \vec{H}_{sc}^* \right) \cdot \hat{n} d\Sigma}{\operatorname{Re} \left(\vec{E}_0 \times \vec{H}_0^* \right)};$$

SCATTERING CROSS SECTION

$$ACS = \frac{P_{ab}}{\mathcal{P}_0} = - \frac{\operatorname{Re} \int_{\Sigma} \left(\vec{E}_{tot} \times \vec{H}_{tot}^* \right) \cdot \hat{n} d\Sigma}{\operatorname{Re} \left(\vec{E}_0 \times \vec{H}_0^* \right)};$$

ABSORPTION CROSS SECTION

$$ECS = \frac{P_{ext}}{\mathcal{P}_0} = - \frac{\operatorname{Re} \int_{\Sigma} \left(\vec{E}_0 \times \vec{H}_{sc}^* + \vec{E}_{sc} \times \vec{H}_0^* \right) \cdot \hat{n} d\Sigma}{\operatorname{Re} \left(\vec{E}_0 \times \vec{H}_0^* \right)};$$

EXTINCTION CROSS SECTION

SECOND HARMONIC GENERATION

$$\vec{E}(\vec{r}, \omega) = \vec{E}_0(\vec{r}, \omega) + \frac{1}{\epsilon_0} \int \vec{S}_0(\vec{r}, \vec{r}', \omega) \cdot \left[\vec{P}(\vec{r}', \omega) + \cancel{\vec{P}^{(2)}(\vec{r}', \omega)} \right] d\vec{r}', \quad \text{FF}$$

$$\vec{E}(\vec{r}, 2\omega) = \frac{1}{\epsilon_0} \int \vec{S}_0(\vec{r}, \vec{r}', 2\omega) \cdot \left[\vec{P}(\vec{r}', 2\omega) + \vec{P}^{(2)}(\vec{r}', 2\omega) \right] d\vec{r}', \quad \text{SH}$$

Where:

$$\begin{aligned} \vec{P}(\vec{r}', \omega) &= \epsilon_0 \chi_b(\vec{r}', \omega) \vec{E}(\vec{r}', \omega), \\ \vec{P}(\vec{r}', 2\omega) &= \epsilon_0 \chi_b(\vec{r}', 2\omega) \vec{E}(\vec{r}', 2\omega), \end{aligned}$$

and:

$$\begin{aligned} \vec{P}^{(2)}(\vec{r}', \omega) &= 2\epsilon_0 \hat{\chi}^{(2)}(\vec{r}', \omega) : \vec{E}(\vec{r}', 2\omega) \vec{E}^*(\vec{r}', \omega), \\ \vec{P}^{(2)}(\vec{r}', 2\omega) &= \epsilon_0 \hat{\chi}^{(2)}(\vec{r}', 2\omega) : \vec{E}(\vec{r}', \omega) \vec{E}(\vec{r}', \omega), \end{aligned}$$

For small objects the nonlinear effects on the fundamental field are negligible at reasonable intensities, thus we ignore the $P^{(2)}$ term at ω . This means that the fundamental field can be calculated by solving the linear equation as previously shown:

SECOND HARMONIC GENERATION

$$\vec{E}(\vec{r}, \omega) = \vec{E}_0(\vec{r}, \omega) + \lim_{V_\delta \rightarrow 0} \int_{V-V_\delta} k_0^2 \chi_b(\vec{r}', \omega) \bar{\bar{G}}_E(\vec{r}, \vec{r}', \omega) \cdot \vec{E}(\vec{r}', \omega) d\vec{r}' - \bar{L} \frac{\chi_b(\vec{r}, \omega)}{\epsilon_b(\omega)} \vec{E}(\vec{r}, \omega),$$

Then we can calculate the second harmonic field inside the object:

$$\vec{E}(\vec{r}, 2\omega) = \lim_{V_\delta \rightarrow 0} \int_{V-V_\delta} k_0^2 \chi_b(\vec{r}', 2\omega) \bar{\bar{G}}_E(\vec{r}, \vec{r}', 2\omega) \cdot \vec{E}(\vec{r}', 2\omega) d\vec{r}' - \bar{L} \frac{\chi_b(\vec{r}, 2\omega)}{\epsilon_b(2\omega)} \vec{E}(\vec{r}, 2\omega) +$$

$$+ \lim_{V_\delta \rightarrow 0} \int_{V-V_\delta} k_0^2 \bar{\bar{G}}_E(\vec{r}, \vec{r}', 2\omega) \cdot \hat{\chi}^{(2)}(\vec{r}', 2\omega) : \vec{E}(\vec{r}', \omega) \vec{E}(\vec{r}', \omega) d\vec{r}' - \bar{L} \frac{\hat{\chi}^{(2)}(\vec{r}, 2\omega)}{\epsilon_b(2\omega)} : \vec{E}(\vec{r}, \omega) \vec{E}(\vec{r}, \omega);$$

The scattered field is similar to the expression for the fundamental field

This term can be calculated by substituting the E field at the FF previously calculated. It acts as a known term:

The discretized equation is:

SECOND HARMONIC GENERATION

$$\vec{E}_{2,i} - \sum_{j=1, j \neq i}^N \overline{\overline{G}}_{i,j}^{(2)} \cdot \left[k_{2,0}^2 \chi_{2,j} \vec{E}_{2,j} \right] \Delta \tau_j - \left(k_{2,0}^2 \overline{\overline{M}}_i^{(2)} \cdot \chi_{2,i} - \overline{\overline{L}} \frac{\chi_{2,i}}{\epsilon_{2,b}} \right) \vec{E}_{2,i} =$$

$$= \sum_{j=1, j \neq i}^N \overline{\overline{G}}_{i,j}^{(2)} \cdot \left[k_{2,0}^2 \widehat{\chi}_j^{(2)} : \vec{E}_{1,j} \vec{E}_{1,j} \right] \Delta \tau_j + \left(k_{2,0}^2 \overline{\overline{M}}_i^{(2)} - \frac{1}{\epsilon_{2,b}} \overline{\overline{L}} \right) \widehat{\chi}_i^{(2)} : \vec{E}_{1,i} \vec{E}_{1,i};$$

The equation can be written in compact form:

$$\left(\overline{\overline{I}} - \overline{\overline{S}} - \overline{\overline{A}} \right) \cdot \overline{\overline{X}} = \overline{\overline{B}}$$

The solution is obtained by the inversion of the K matrix :

$$\overline{\overline{K}} \cdot \overline{\overline{X}} = \overline{\overline{B}} \quad \Longrightarrow \quad \overline{\overline{X}} = \overline{\overline{K}}^{-1} \cdot \overline{\overline{B}}$$

SECOND HARMONIC GENERATION IN METAL NANOPARTICLES

The nonlinear polarization density is due to magnetic dipole and electric quadrupole contributions:

$$\mathbf{P}^{\text{NL}}(\mathbf{r}|2\omega) = \alpha[\mathbf{E}(\mathbf{r}|\omega) \cdot \nabla]\mathbf{E}(\mathbf{r}|\omega) + \beta\mathbf{E}(\mathbf{r}|\omega) \times [\nabla \cdot \mathbf{E}(\mathbf{r}|\omega)] + \gamma\nabla[\mathbf{E}(\mathbf{r}|\omega) \cdot \mathbf{E}(\mathbf{r}|\omega)]$$

where $\alpha = \delta - \beta - 2\gamma$

δ, β, γ are frequency dependent parameters characterizing the medium

SHG originates from both bulk and surface response.

The parameters can be estimated by modeling the optical response of the material. For example in the case of metals several models have been proposed:

Free electron gas model

F. Brown, R. E. Parks, and A. M. Sleeper, Phys. Rev. Lett. 14, 1029 1965.

N. Bloembergen, R. K. Chang, and C. H. Lee, Phys. Rev. Lett. 16, 986–989 (1966);

Hydrodynamic Model

J. E. Sipe and G. I. Stegeman, in *Surface Polaritons: Electromagnetic Waves at Surfaces and Interfaces*, edited by V.M.Agranovich and D. L. Mills North-Holland, Amsterdam, 1982.

Nonlinear quantum mechanical surface response of conduction electrons is calculated with the jellium model.

A. Liebsch, Phys. Rev. Lett. 61, 10 1988

A. Liebsch, *Electronic Excitations at Metal Surfaces* Plenum, New York, 1997.

Drude-Lorentz Model for the Optical Response of Metals

We begin by assuming that at optical frequencies the linear response of a metal is strongly affected by the bound valence electrons.

$$\epsilon_r(\omega) = \epsilon_D(\omega) + \sum_{j=1}^5 \frac{G_j \omega_p^2}{\omega_{0,j}^2 - \omega^2 - i\omega\kappa_j}$$

$$\epsilon_D(\omega) = 1 - \frac{\omega_0^2}{\omega^2 - i\omega\kappa_0}$$

ϵ_D is the electric permittivity obtained by considering the Drude model only.
 ω_p is the plasma frequency
 G_j and $\omega_{0,j}$ respectively are the oscillator strengths and resonant frequencies,
 κ_j are damping constants related to each oscillator.
 ω_0 is the plasma frequency associated with intraband transitions
 (related only to the free electron density) with oscillator strength G_0 and damping constant κ_0 .

A.D. Rakic', A. B. Djuris' ic', J. M. Elazar and M. L. Majewski, *Appl. Opt.*, Vol. 37, No. 22 (1998).

we model the optical response of the metal by assuming an effective current density:

$$\vec{J} = \vec{J}_D + \frac{\partial \vec{P}_{b.e.}}{\partial t}$$

where \vec{J}_D is the current density induced by the electromagnetic field on the free electrons and $\vec{P}_{b.e.}$ is the polarization vector due to the presence of bound electrons. Each term contains both linear and nonlinear contributions. **At this stage we consider nonlinear effects related to the response of conduction electrons only.**

Evaluation of Bulk and Surface contributions

We separate bulk and surface contributions

$$\vec{J}_{NL}^{Bulk} = -i2\omega \left[\gamma \delta' (\vec{E}_1 \cdot \vec{\nabla}) \vec{E}_1 + \gamma d \vec{\nabla} [\vec{E}_1 \cdot \vec{E}_1] \right];$$

Bulk nonlinear term driven by absorption losses. It is not present in the classical free electron gas theory

$$\hat{X} \cdot \vec{J}_{NL}^{Surface} = -i2\omega (4\gamma b) E_{1,X}^{(-)} E_{1,Y}^{(-)} \delta(Y);$$

$$\hat{Y} \cdot \vec{J}_{NL}^{Surface} = -i2\omega (2\gamma a) [E_{1,Y}^{(-)}]^2 \delta(Y);$$

$$\hat{Z} \cdot \vec{J}_{NL}^{Surface} = -i2\omega (4\gamma b) E_{1,Z}^{(-)} E_{1,Y}^{(-)} \delta(Y);$$

$$d = \alpha\beta;$$

$$\delta' = 2\alpha\beta(\alpha - 1);$$

$$b = -\alpha^2\beta;$$

$$\gamma = \frac{e\epsilon_0\omega_0^2}{8m\omega^4}$$

$$a = -\alpha^2\beta \frac{(\epsilon_{r,\omega} + 3)}{2};$$

$$\alpha = \frac{\omega}{\omega + i\kappa_0}; \quad \beta = \frac{2\omega}{2\omega + i\kappa_0};$$

The field is evaluated inside the object when the distance to the boundary tends to zero

$\hat{X}(\vec{r}')$ and $\hat{Y}(\vec{r}')$ are the local unit vectors tangential and normal (outgoing) to the surface

Numerical evaluation of generated second harmonic field

The generated field pattern can be calculated by considering the equation for the generated SH electric field:

$$\left(\vec{\nabla} \wedge \vec{\nabla} \wedge - \frac{(2\omega)^2}{c^2} \bar{\bar{I}} \right) \vec{E}_2(\vec{r}) = i(2\omega) \vec{J}_2(\vec{r});$$

being:

$$\vec{J}_2(\vec{r}) = -i2\omega\epsilon_0\chi_{b,2}(\vec{r})\vec{E}_2(\vec{r}) + \vec{J}_{NL}^{Bulk}(\vec{r}) + \vec{J}_{NL}^{Surface}(\vec{r});$$

The formal solution is:

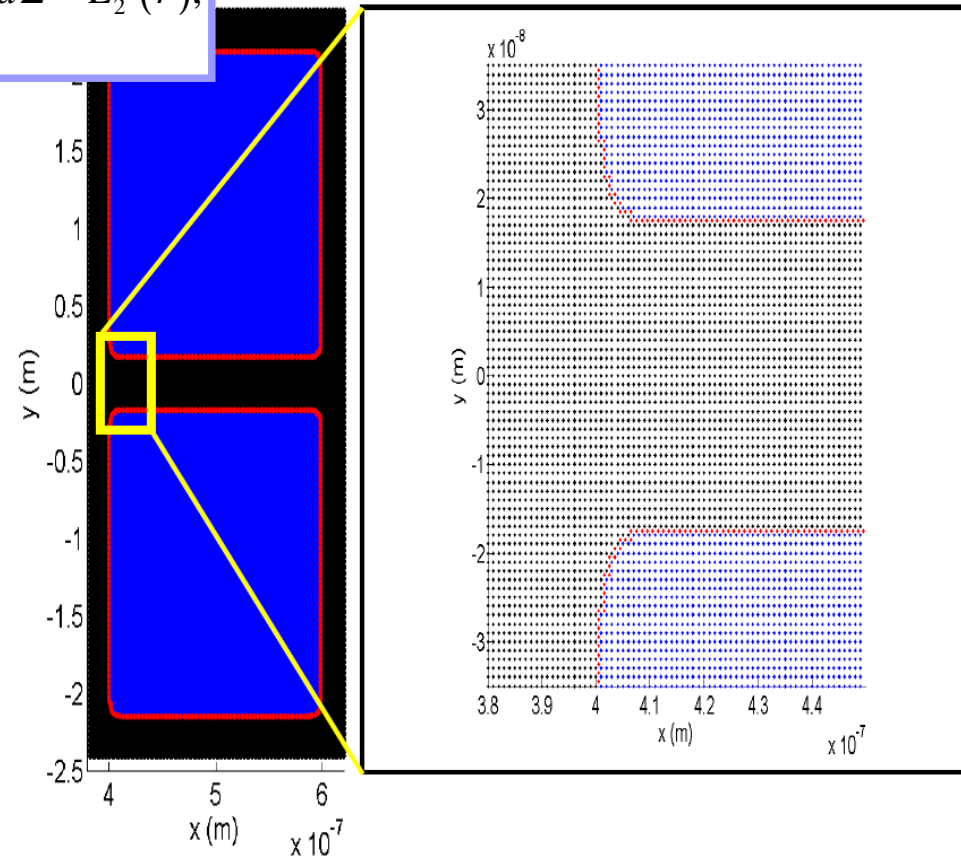
$$\begin{aligned} \vec{E}_2(\vec{r}) = & \lim_{V_\delta \rightarrow 0} \int_{V-V_\delta} k_0^2 \chi_{b,2}(\vec{r}') \bar{\bar{G}}_E(\vec{r}, \vec{r}', 2\omega) \cdot \vec{E}_2(\vec{r}') d\vec{r}' - \bar{\bar{L}} \frac{\chi_{b,2}(\vec{r})}{\epsilon_{b,2}} \vec{E}_2(\vec{r}) + \\ & + i2\omega \lim_{V_\delta \rightarrow 0} \int_{V-V_\delta} \bar{\bar{G}}_E(\vec{r}, \vec{r}', 2\omega) \cdot \vec{J}_{NL}^{Bulk}(\vec{r}') d\vec{r}' - \frac{i}{2\omega\epsilon_0\epsilon_{b,2}} \bar{\bar{L}} \cdot \vec{J}_{NL}^{Bulk}(\vec{r}) + \\ & + i2\omega \int_V \bar{\bar{G}}_E(\vec{r}, \vec{r}', 2\omega) \cdot \vec{J}_{NL}^{Surface}(\vec{r}') d\vec{r}'; \end{aligned}$$

Numerical evaluation of generated second harmonic field

the nonlinear surface term reduces to a surface (2D) integral along the boundary of V (named Σ) when the expression of the surface current density is considered:

$$\int_V \overline{\overline{G_E}}(\vec{r}, \vec{r}') \vec{J}_{NL}^{Surface}(\vec{r}') d\tau' = \int_{\Sigma} \overline{\overline{G_E}}(\vec{r}, \Sigma) \vec{J}(\Sigma) d\Sigma = \vec{E}_2^{\Sigma}(\vec{r});$$

Boundary points are not considered as scattered points. The calculation of the integral can be performed without introducing other terms and its value is considered as an impressed field.



SECOND HARMONIC GENERATION

$$\vec{E}_{2,i} - \sum_{j=1, j \neq i}^N \overline{\overline{G}}_{i,j}^{(2)} \cdot \left[k_{2,0}^2 \overline{\overline{\chi}}_{2,j} \vec{E}_{2,j} \right] \Delta \tau_j - \left(k_{2,0}^2 \overline{\overline{M}}_i^{(2)} \cdot \overline{\overline{\chi}}_{2,i} - \overline{\overline{L}} \frac{\overline{\overline{\chi}}_{2,i}}{\overline{\overline{\epsilon}}_{2,b}} \right) \vec{E}_{2,i} =$$

$$= i2\omega_0 \left[\sum_{j=1, j \neq i}^N \overline{\overline{G}}_{i,j}^{(2)} \cdot \vec{J}_{NL,j}^{Buk} \Delta \tau_j + \left(\overline{\overline{M}}_i^{(2)} - \frac{1}{k_{2,0}^2 \overline{\overline{\epsilon}}_{2,b}} \overline{\overline{L}} \right) \vec{J}_{NL,i}^{Buk} \right] + \vec{E}_{2,i}^{\Sigma};$$

The equation can be written in compact form:

$$\left(\overline{\overline{I}} - \overline{\overline{S}} - \overline{\overline{A}} \right) \cdot \overline{\overline{X}} = \overline{\overline{B}}$$

The solution is obtained by the inversion of the K matrix :

$$\overline{\overline{K}} \cdot \overline{\overline{X}} = \overline{\overline{B}} \implies \overline{\overline{X}} = \overline{\overline{K}}^{-1} \cdot \overline{\overline{B}}$$

Stratified backgrounds

PHYSICAL REVIEW E, VOLUME 63, 066615

Green's tensor technique for scattering in two-dimensional stratified media

Michael Paulus^{1,2} and Olivier J. F. Martin^{1,*}

¹*Electromagnetic Fields and Microwave Electronics Laboratory, Swiss Federal Institute of Technology, ETH-Zentrum ETZ, CH-8092 Zurich, Switzerland*

²*IBM Research, Zurich Research Laboratory, CH-8803 Rüschlikon, Switzerland*

(Received 1 February 2001; published 29 May 2001)

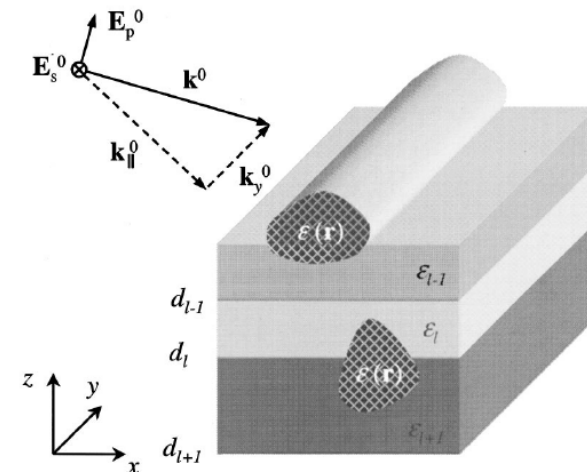
The procedure is the same as described before but the Green tensor for a stratified background must be used:

While there is an analytical expression for the Green tensor in a homogenous medium, it is not possible to evaluate the Green tensor for a stratified medium analytically.

Nevertheless it is possible to evaluate it numerically:

M. Paulus, P. Gay-Balmaz,¹ and O. J. F. Martin, "Accurate and efficient computation of the Green's tensor for stratified media" Phys. Rev. E, 62, 4, (2000)

Tatsuo Itoh Ed. " Numerical Techniques for microwave and millimeter wave passive structures" Wiley ad Sons (1989)



CONCLUSIONS (numerical model)

ADVANTAGES

Simple implementation,
it does not require discretization of the entire space,
only the objects need to be discretized, it can easily handle systems
composed by nanoparticles on top of layered structures.

The field can be evaluated everywhere in the space once it is known the field
inside the object.

Useful for investigating near field as well as far field properties.

DRAWBACKS

High dielectric permittivity scatterers require a fine mesh.

All the data are stored in matrices requiring a big amount of available RAM.

Matrix inversion might be heavy to compute.

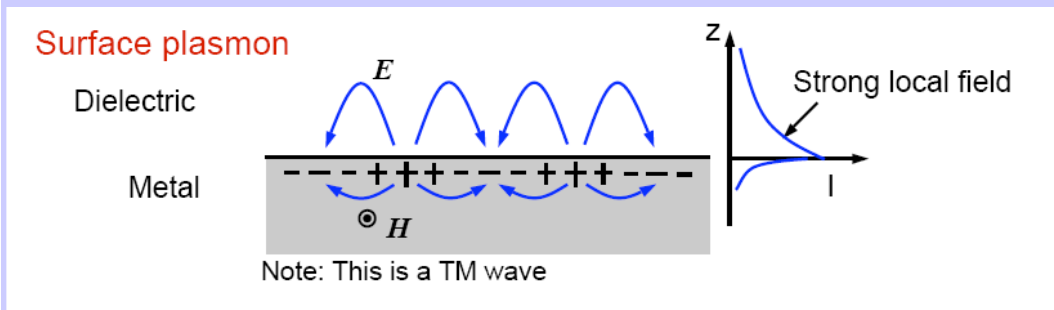
EXAMPLES

Nonlinear frequency conversion at the nanoscale: Main features

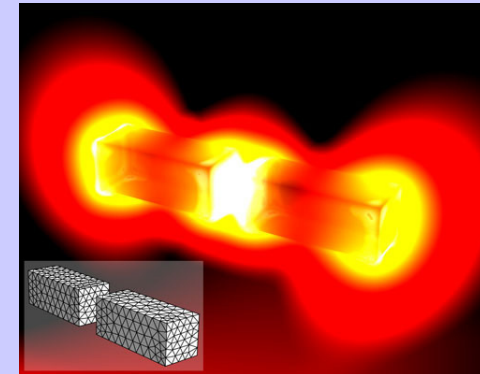
If the field is confined and localized in subwavelength regions **phase mismatch does not play a crucial role.**

On the other hand, **overlap between fundamental frequency field and second harmonic field is important.** Optimal conditions are achieved if both fields are localized in order to maximize the overlap.

Sub wavelength field localization can be achieved by excitation of surface plasmon polariton and localized surface plasmon polariton at metal dielectric interface.



Strong field confinement across the surface.
Evanescent waves in the metal and in the dielectric



[Fisher and Martin, Opt. Express 16, 9144-9154 (2008)].

Optical second-harmonic generation with surface plasmons in noncentrosymmetric crystals

J. G. Rako, J. C. Quail, and H. J. Simon
 Department of Physics and Astronomy, The University of Toledo, Toledo, Ohio 43606
 (Received 23 January 1984)

J. Appl. Phys., Vol. 56, No. 9, 1 November 1984

Second-harmonic generation with phase-matched long-range and short-range surface plasmons

J. C. Quail and H. J. Simon
 Department of Physics and Astronomy, The University of Toledo, 1
 (Received 26 April 1984; accepted for publication 18 June 1984)

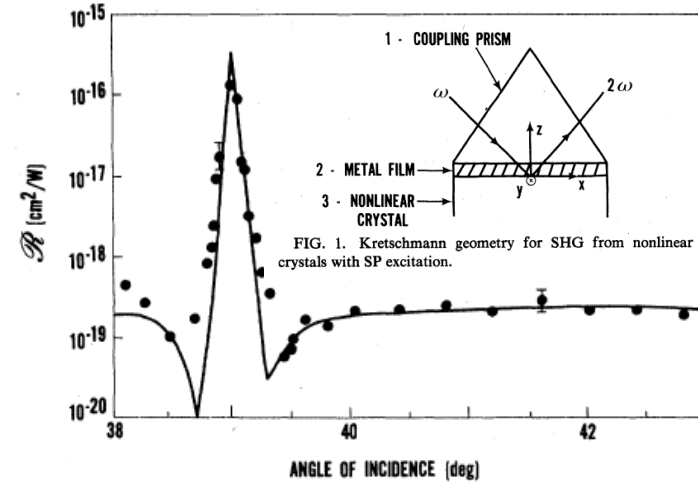
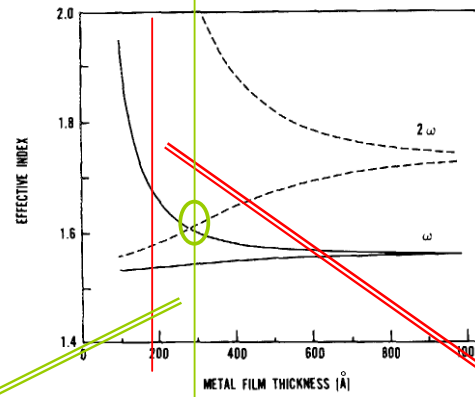


FIG. 2. Reflected SHG (R) vs interior angle of incidence for rutile prism/550-Å-thick Ag film/X-cut quartz in standard experiment. Normalization to theoretical solid curve as discussed in text.

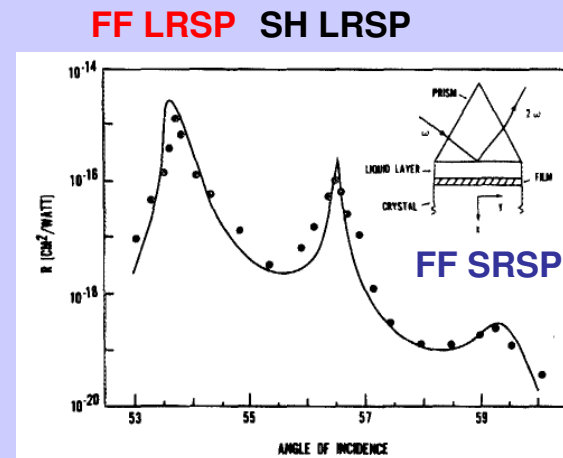
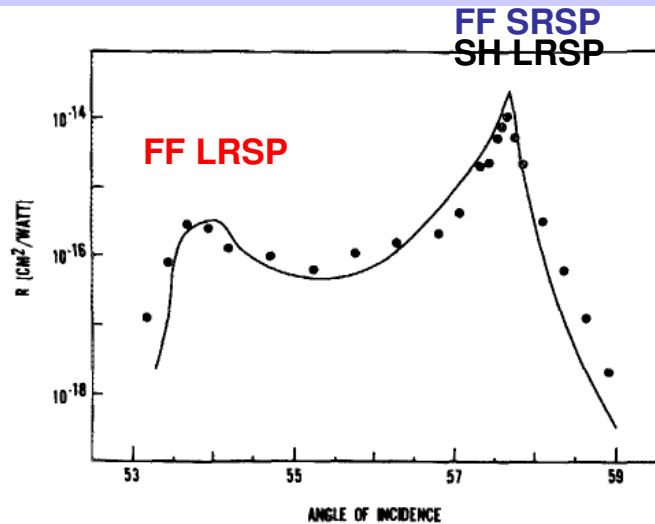


FIG. 2. Second-harmonic reflection coefficient R demonstrating excitation of the fundamental LRSP, harmonic LRSP, and fundamental SRSP modes vs the interior angle of incidence. Inset shows prism geometry.

Electromagnetic theory of diffraction in nonlinear optics and surface-enhanced nonlinear optical effects

R. Reinisch

Laboratoire de Génie Physique, Equipe (No. 836) de Recherche associée au Centre National de La Recherche Scientifique, Ecole Nationale Supérieure d'Ingénieurs Electriciens de Grenoble, Boîte Postale 46, F-38402 Saint-Martin-d'Hères, France

M. Nevière

Laboratoire d'Optique Electromagnétique, Equipe (No. 597) de Recherche associée au Centre National de la Recherche Scientifique, Faculté des Sciences et Techniques, Centre de Saint Jérôme, F-13 397 Marseille Cedex 13, France
(Received 2 June 1982; revised manuscript received 15 November 1982)

Enhancement of the Second order response of metal

Second-harmonic generation in reflection from a metallic grating

G. A. Farias* and A. A. Maradudin

Department of Physics, University of California, Irvine, California 92717
(Received 26 January 1984)

Enhancement of the Second order response of quartz

Second-harmonic generation with surface plasmons from a silvered quartz grating

H. J. Simon, C. Huang, J. C. Quail, and Z. Chen*

Department of Physics and Astronomy, The University of Toledo, Toledo, Ohio 43606
(Received 1 April 1988)

Renewed interest due to development of metamaterials and nanotechnologies

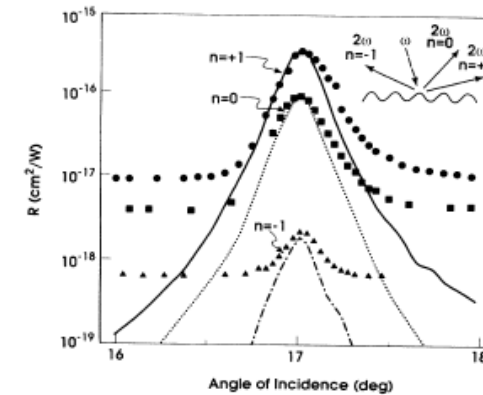
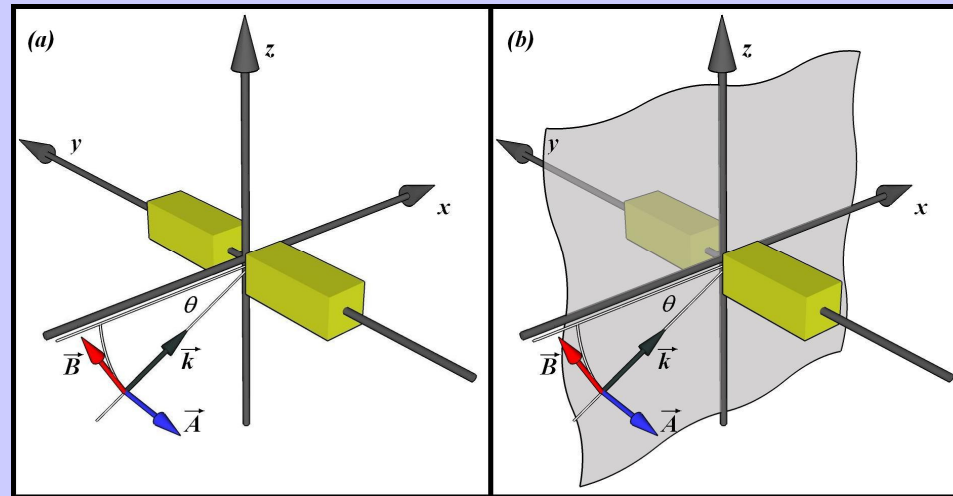


FIG. 5. Nonlinear reflectance on a logarithmic scale for the diffracted SHG modes vs the angle of incidence. Circles, squares, and triangles are experimental points and solid, dotted, and dashed lines are the theoretical curves for the $n = 1, 0,$ and -1 modes, respectively.

Numerical analysis: Linear properties

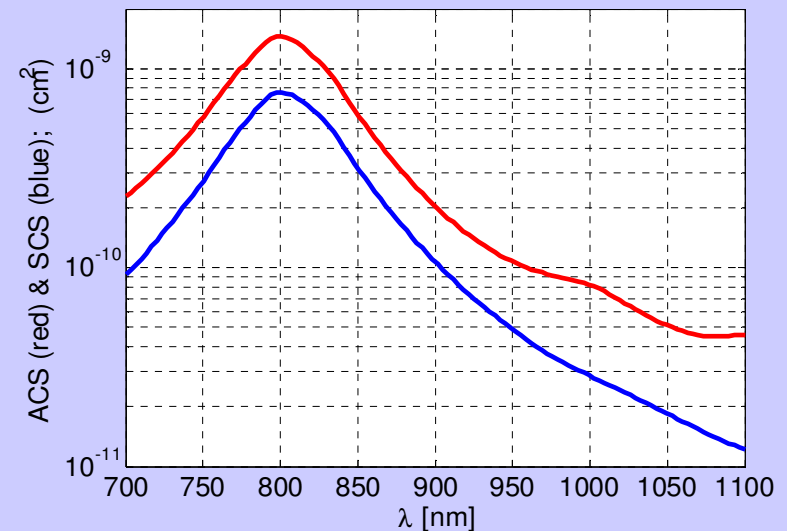


length of each element of the nanoantenna is 100 nm,
 gap between elements is 30 nm.
 Variable cross section thickness
 from $(10 \times 10) \text{ nm}^2$ to $(36 \times 36) \text{ nm}^2$.

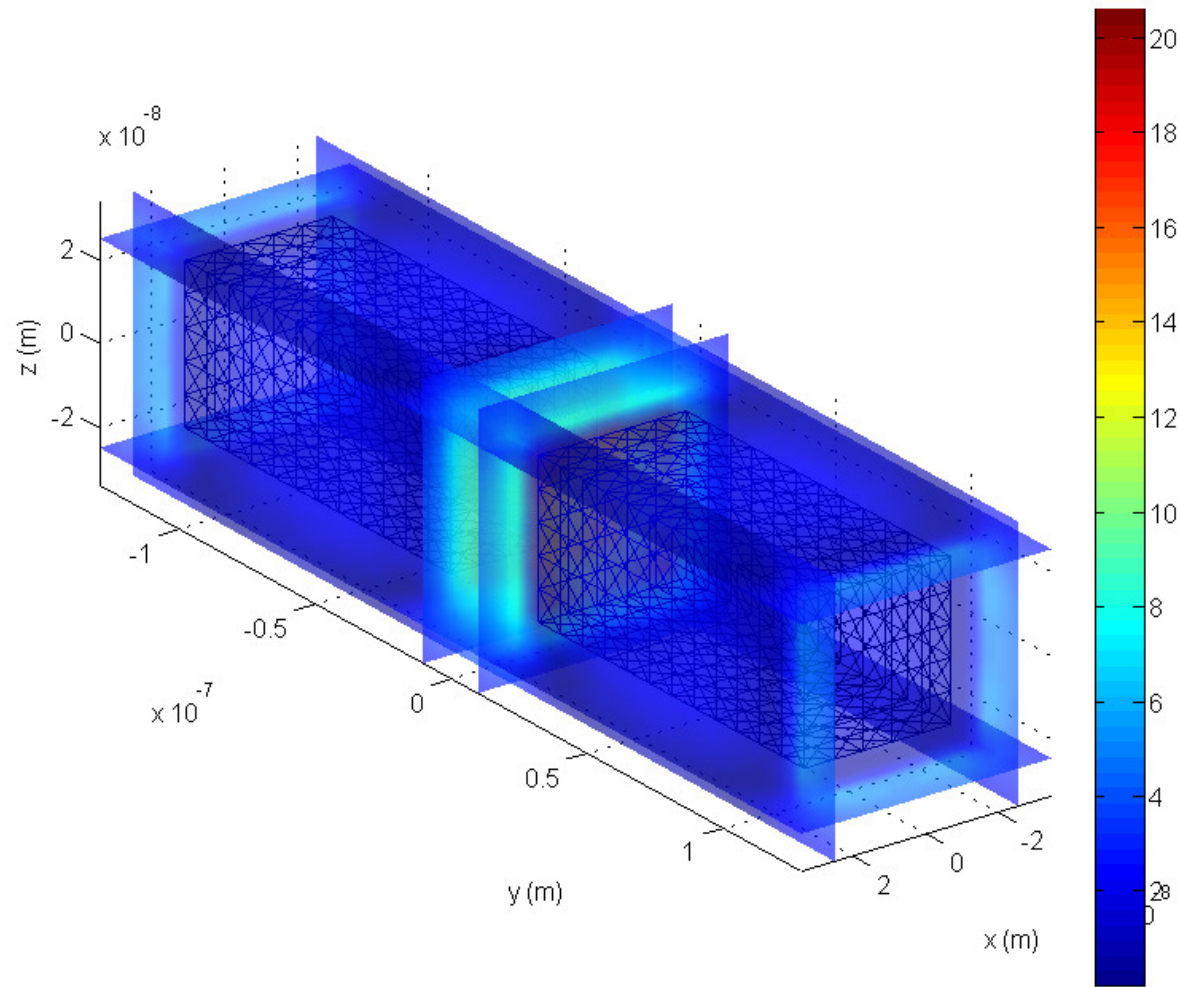
$$ACS = \frac{-\int \text{Re}(\vec{E}_\omega \times \vec{H}_\omega^*) \cdot \hat{n} dS}{\text{Re}(\vec{E}_{0,\omega} \times \vec{H}_{0,\omega}^*)}$$

$$SCS = \frac{\int \text{Re}(\vec{E}_{SC,\omega} \times \vec{H}_{SC,\omega}^*) \cdot \hat{n} dS}{\text{Re}(\vec{E}_{0,\omega} \times \vec{H}_{0,\omega}^*)}$$

$(24 \times 24) \text{ nm}^2$ TE (y) pol

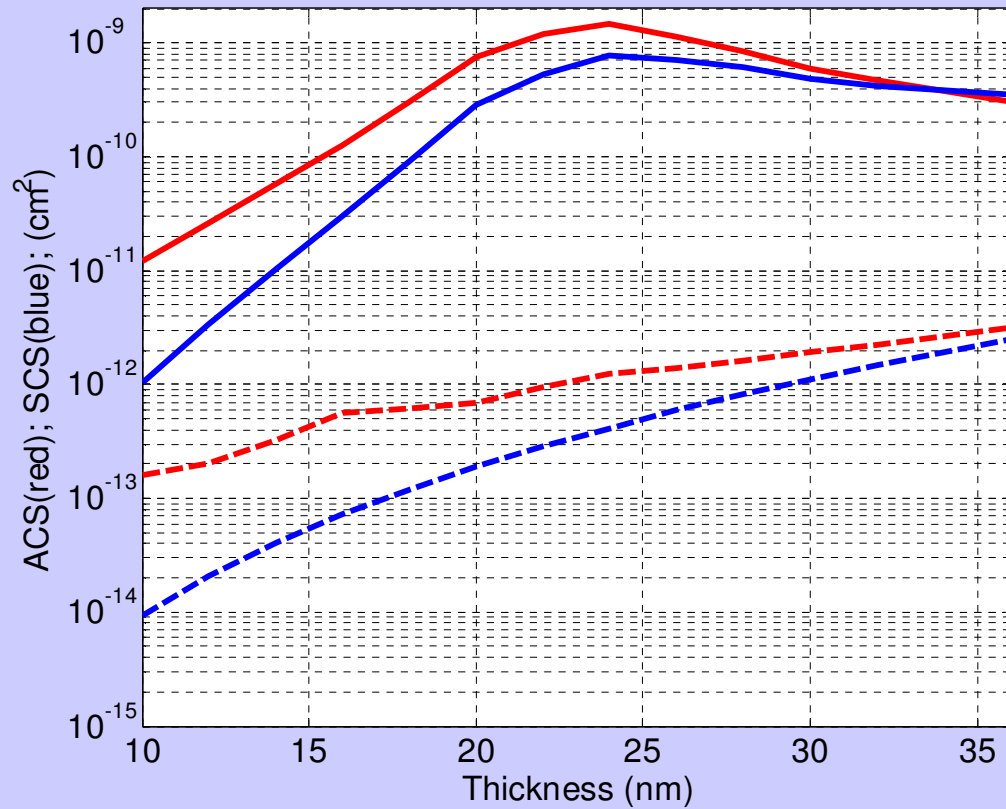


FF $|E_y|/|E_y(\text{inc})|$



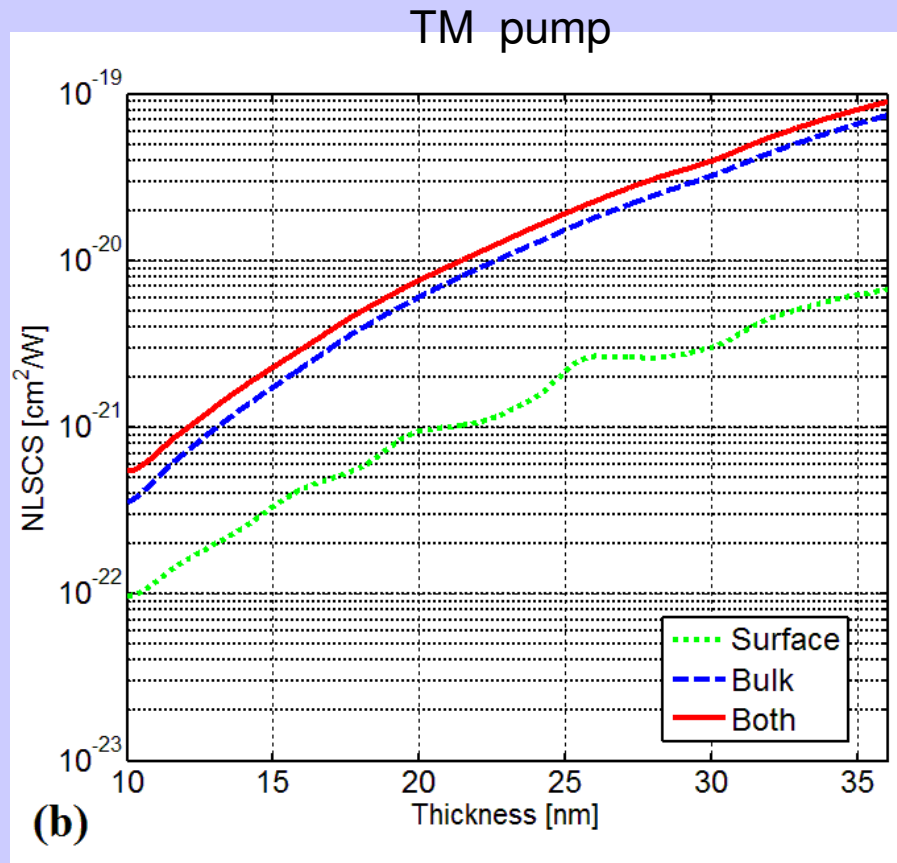
Numerical analysis: Linear properties

Different behavior between TE (y) and TM (z) polarization



(ACS- red curve)
(SCS- blue curve)
TE pol (solid)
TM pol (dashed)

Numerical analysis: Nonlinear properties

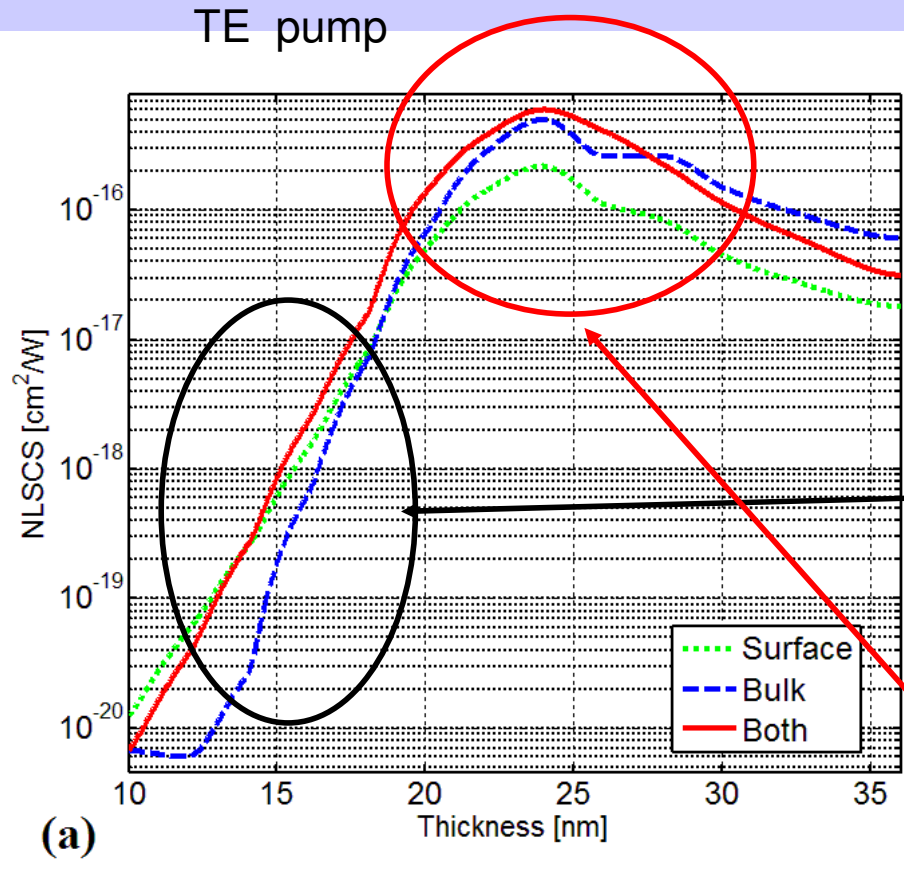


$$NLSCS = \int_S \sigma(\theta, \varphi) d\Omega;$$

$$\sigma(\theta, \varphi) = \frac{2S_{inc} \cdot \text{Re}(\vec{E}_{SC,2\omega} \times \vec{H}_{SC,2\omega}^*) \cdot \hat{n} \cdot R^2}{P_{0,\omega}^2};$$

For TM pump, there are negligible effects due to field localization because the antenna is out of resonance. The SH signal is mostly generated by bulk contributions.

Numerical analysis: Nonlinear properties

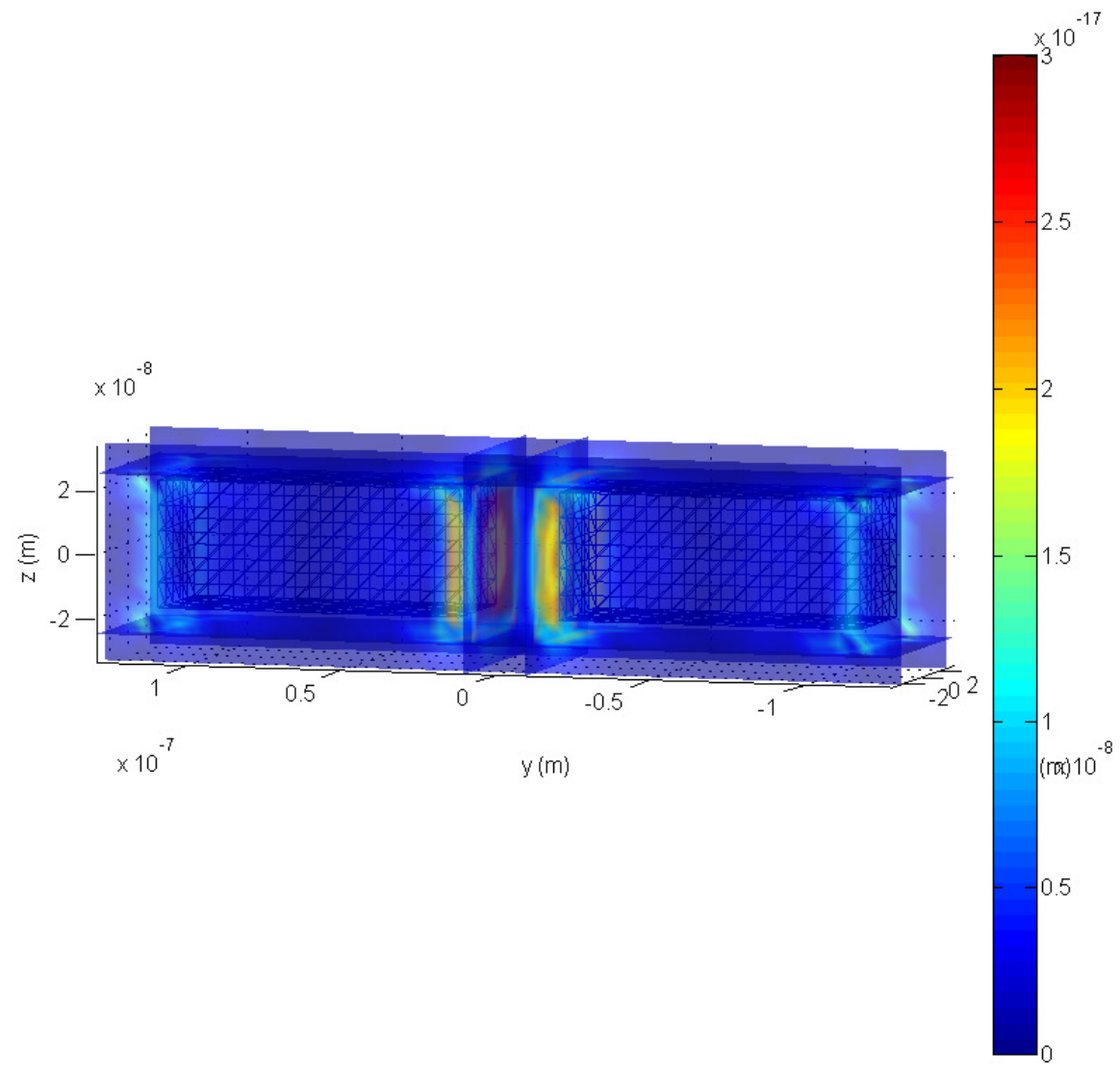


the linear response of the system is stronger with respect to the TM case. High localization of the pump field at metal/air interfaces, higher absorption means higher field penetration inside the metal.

Surface contributions are stronger, as expected for a film.

Pump field becomes more localized close to the air gap between the two rods and at the antenna's tips, reducing the amount of surface effectively contributing to the process and enhancing the bulk nonlinear response

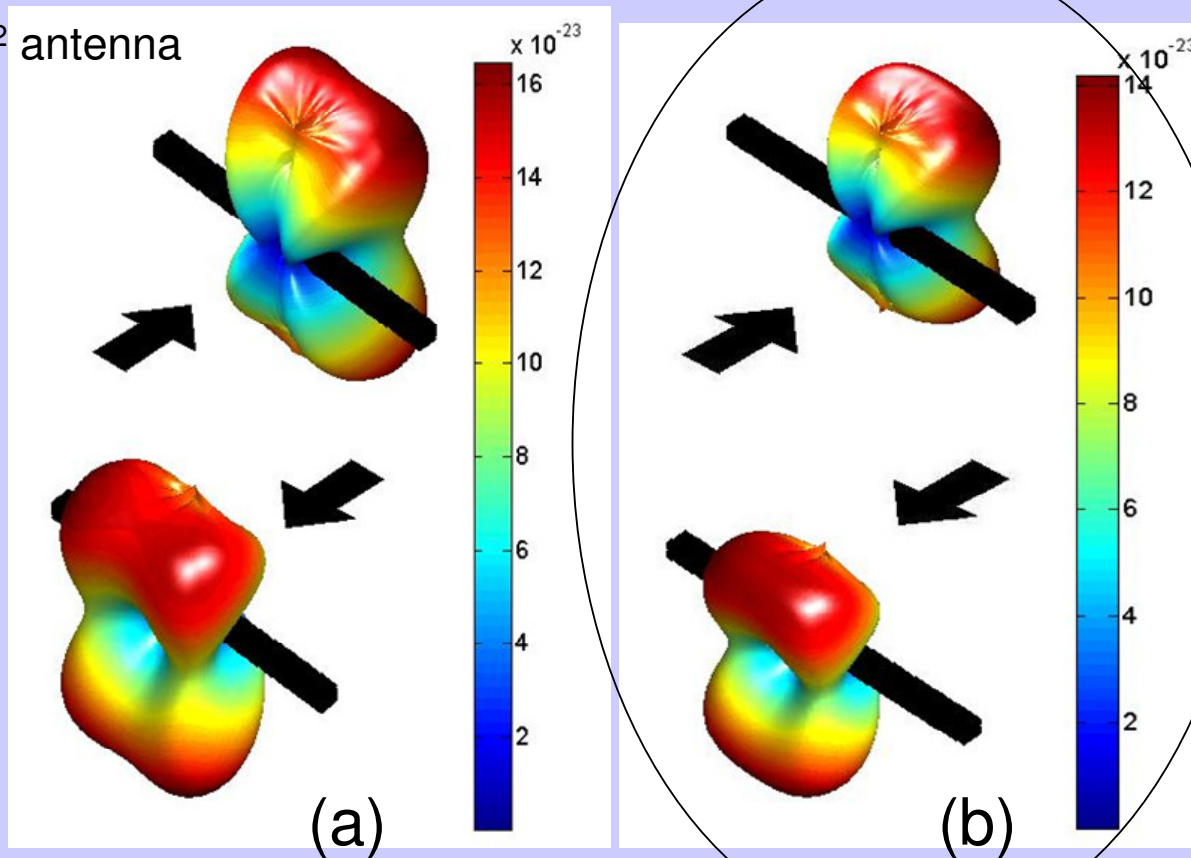
SH $|E_y|$ (a.u.)



Numerical analysis: Far field pattern

Second harmonic differential scattering cross section [cm^2/W] for TM pump

(13x13) nm^2 antenna



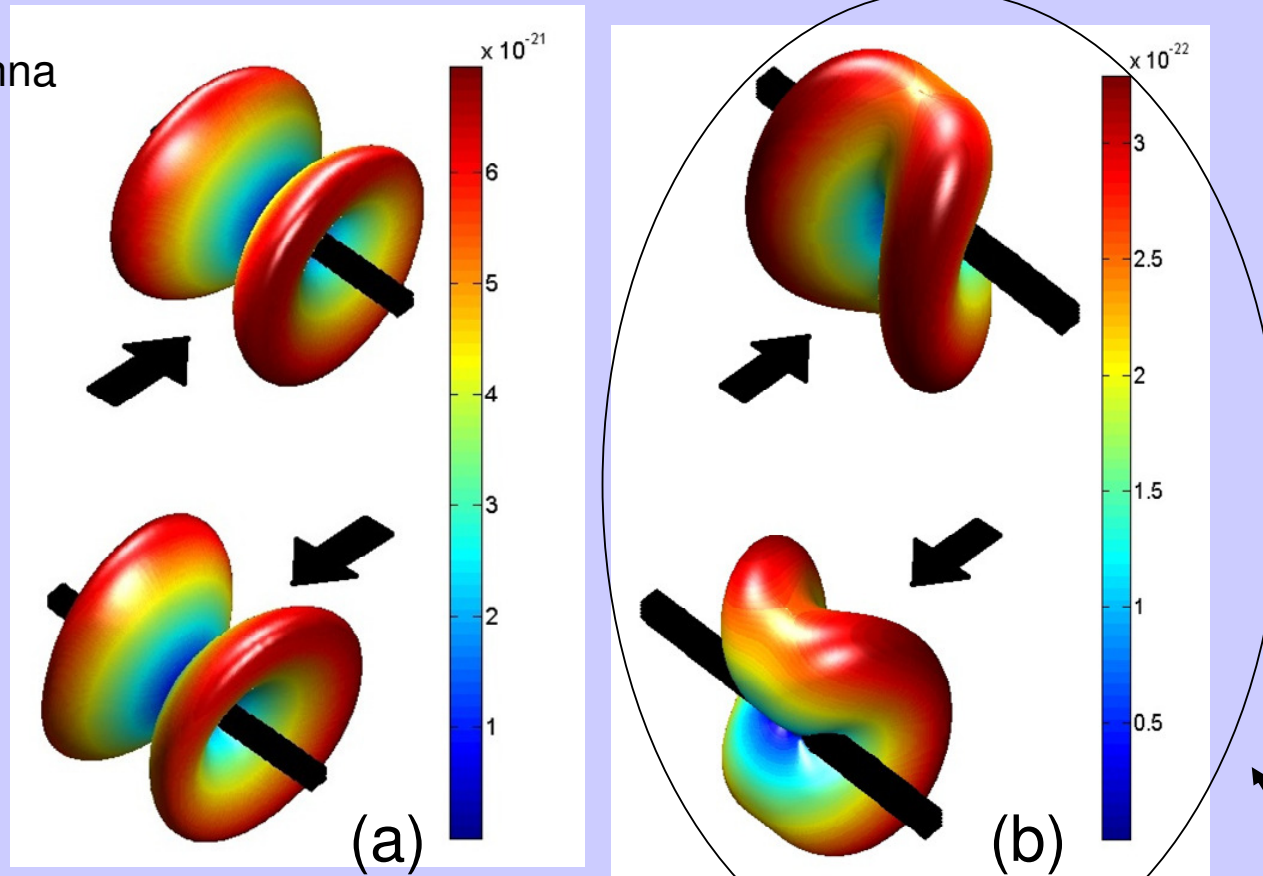
Surface terms can be neglected. Measured signal can be considered only coming from bulk contributions

Only bulk nonlinear contributions

Numerical analysis: Far field pattern

Second harmonic differential scattering cross section [cm^2/W] for TE pump

(13x13) nm^2 antenna



Only bulk nonlinear contributions

Benedetti A; Centini M; Bertolotti M; Sibilìa C, Second harmonic generation from 3D nanoantennas: on the surface and bulk contributions by far-field pattern analysis OPTICS EXPRESS (2011) 19, 26752

Numerical analysis(FF)

Pump at 800 nm, p-pol and normal incidence
(k is parallel to x -axis and \mathbf{E} is parallel to y -axis)

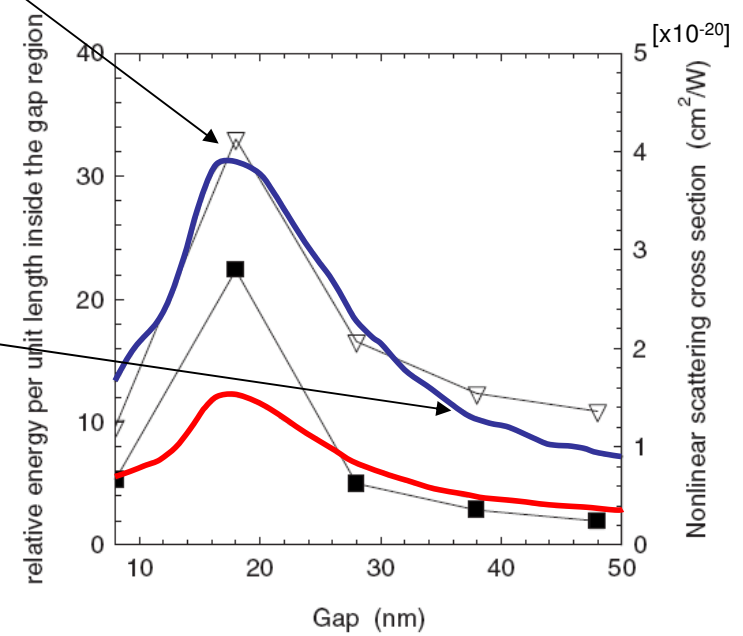
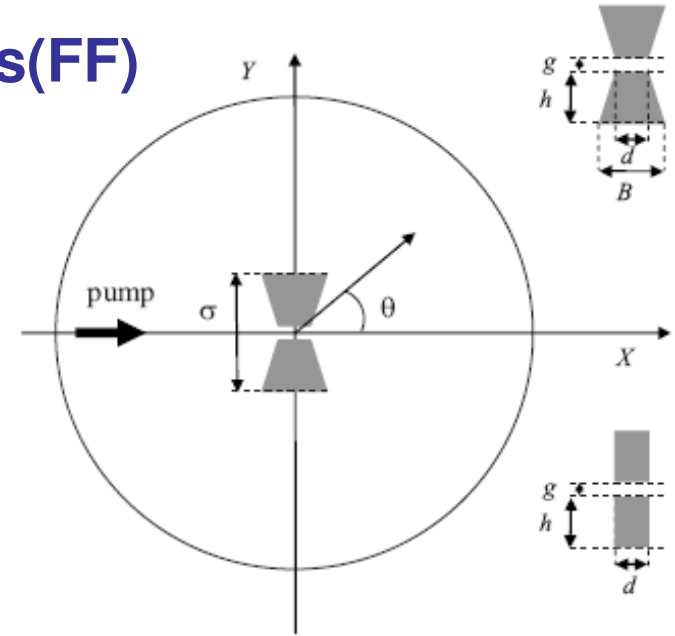
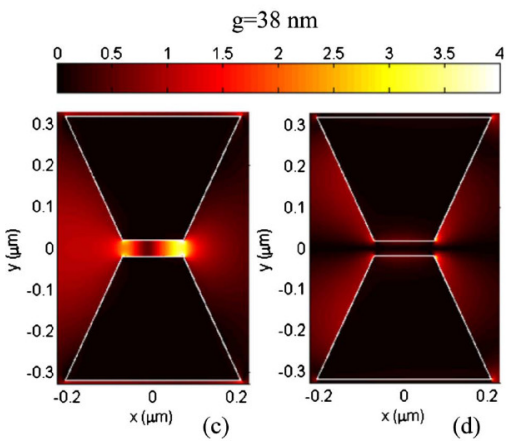
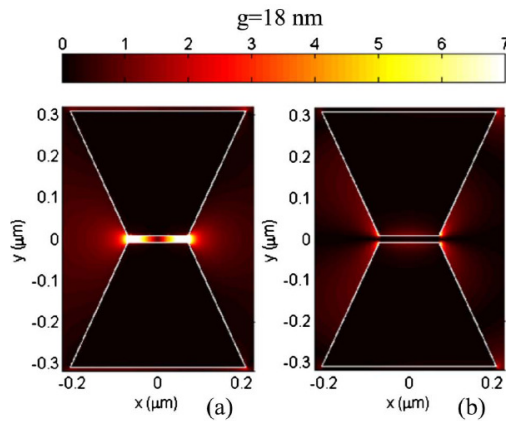
Rectangu

Trapezoid

Average en
region of A

$$W = \int_{gap} \left[\epsilon_0 \right]$$

$$\vec{H}_{1(inc)}(x, y)$$



Numerical analysis (SH)

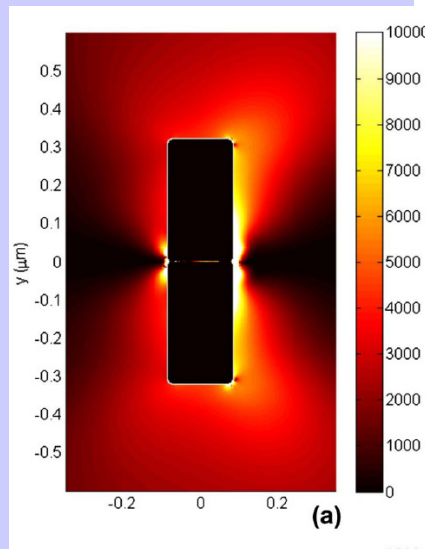
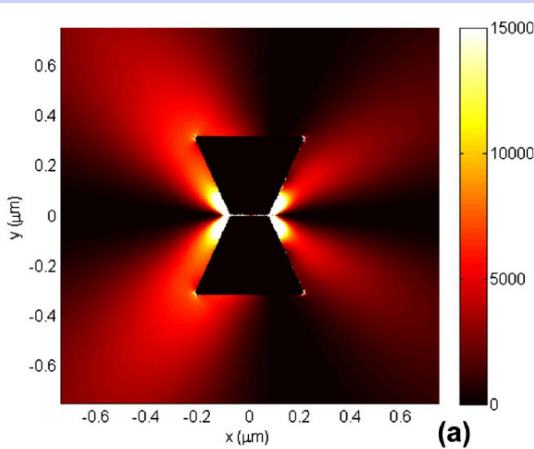
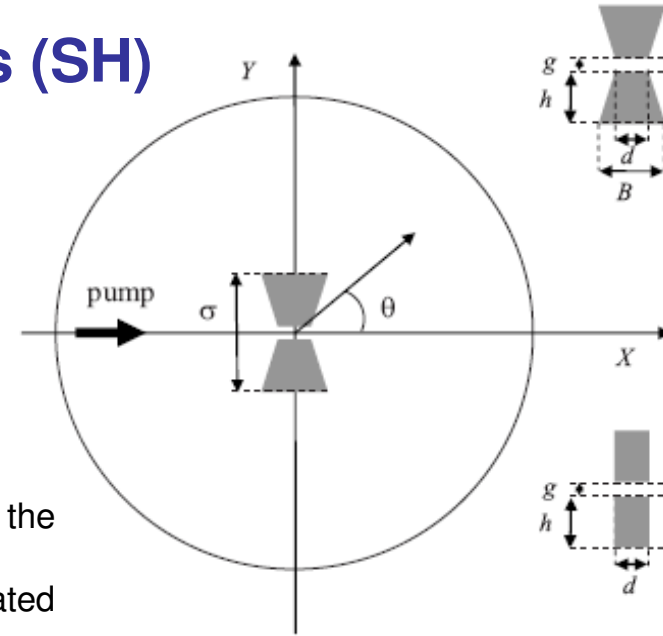
We evaluate the nonlinear scattering cross section $Q(\omega)$:

$$Q(2\omega) = \sigma \frac{P(2\omega)_{sc}}{[P(\omega)_{inc}]^2} = \int_0^{2\pi} q(\theta|2\omega) d\theta;$$

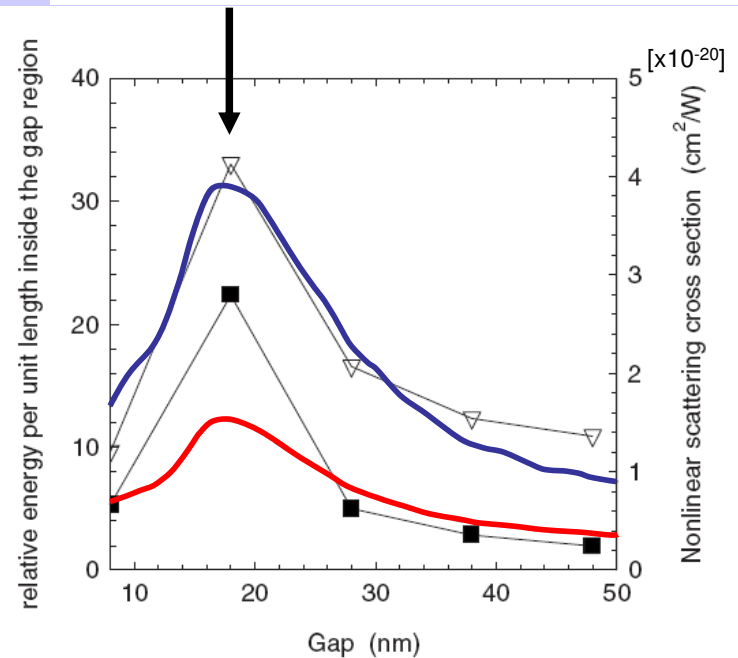
$q(\theta|2\omega)$ is the differential scattering cross section;

$P(\omega)_{inc}$ is the power flow per unit length (W/m) of the FF field across the segment σ

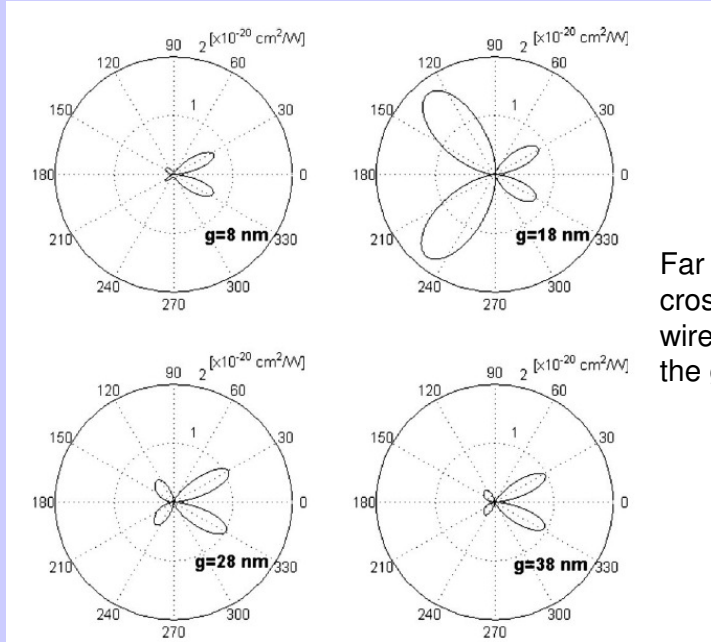
$P(2\omega)_{sc}$ is the generated SH power flow per unit length calculated across a circumference of radius $R \gg \lambda$.



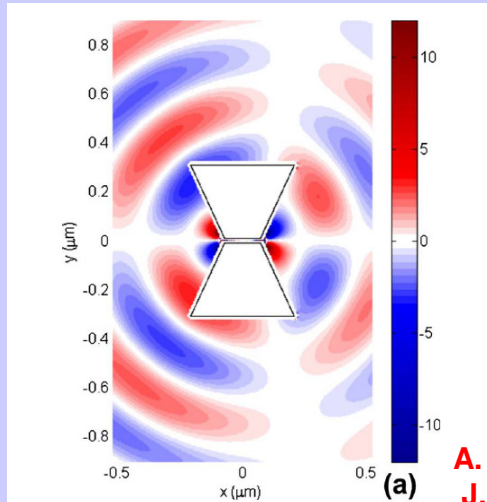
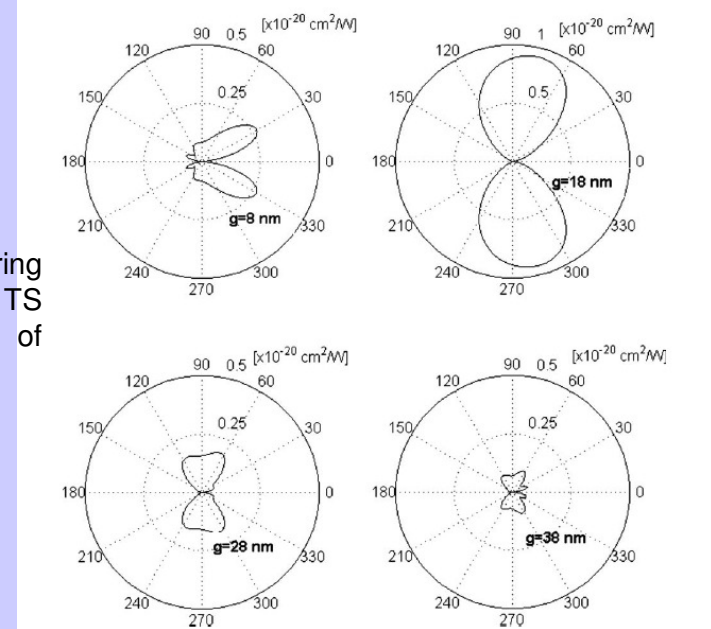
Modulus of the Poynting vector (W/m²)



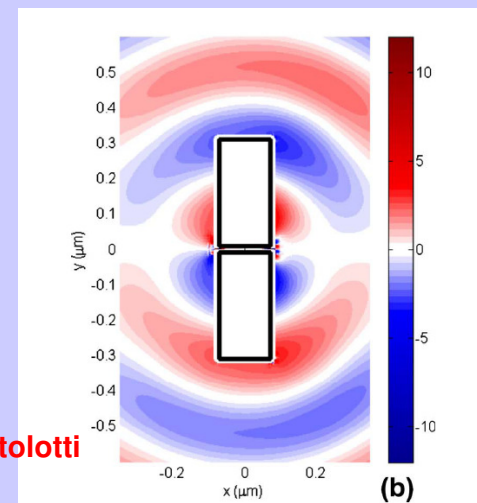
Numerical analysis (SH)



Far field differential scattering cross sections for RS and TS wires for different values of the gap between wires



Real part of the magnetic field H_z (A/m) at the second harmonic frequency for $g=18$ nm

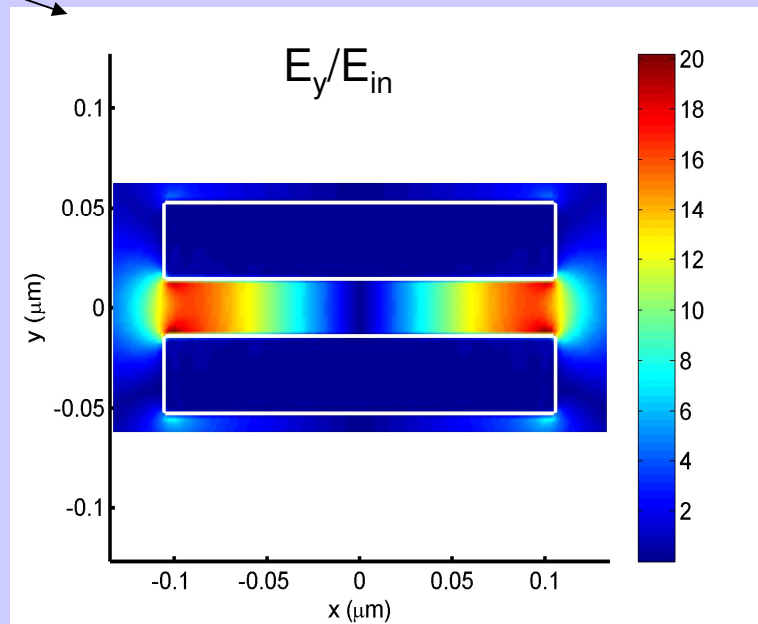
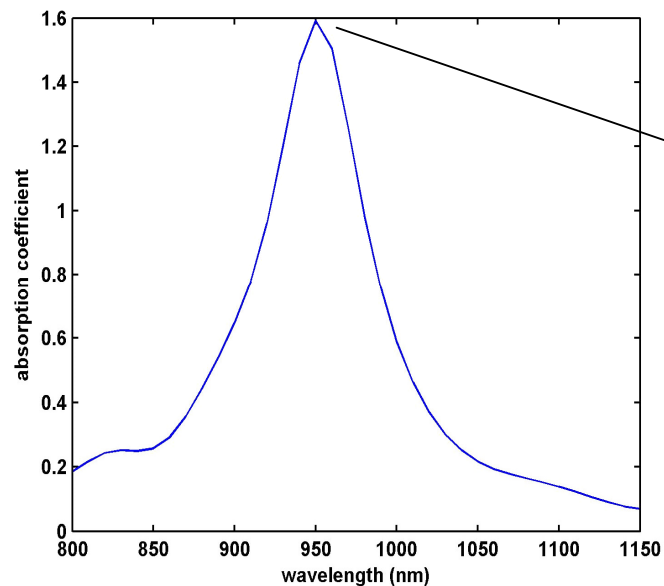
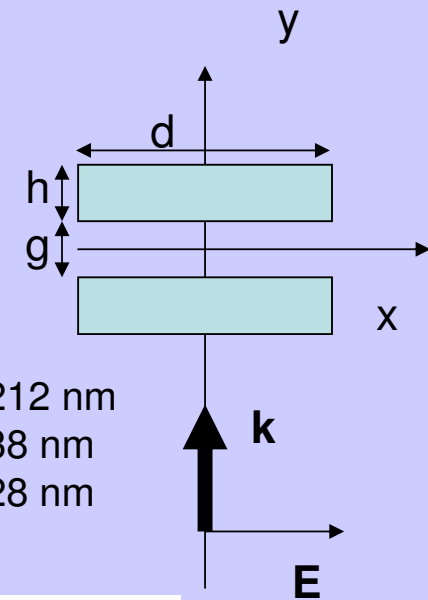


A. Benedetti, M. Centini, C. Sibia, M. Bertolotti
 J. Opt. Soc. Am. B Vol. 27, No. 3, 2010

Silver Coupled Resonators

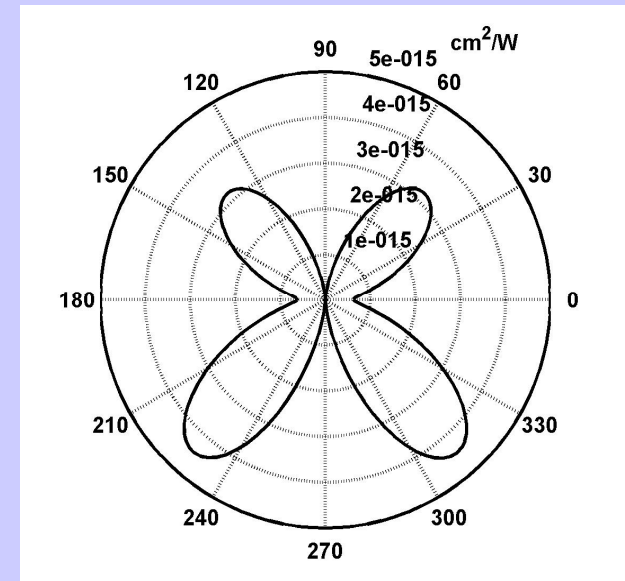
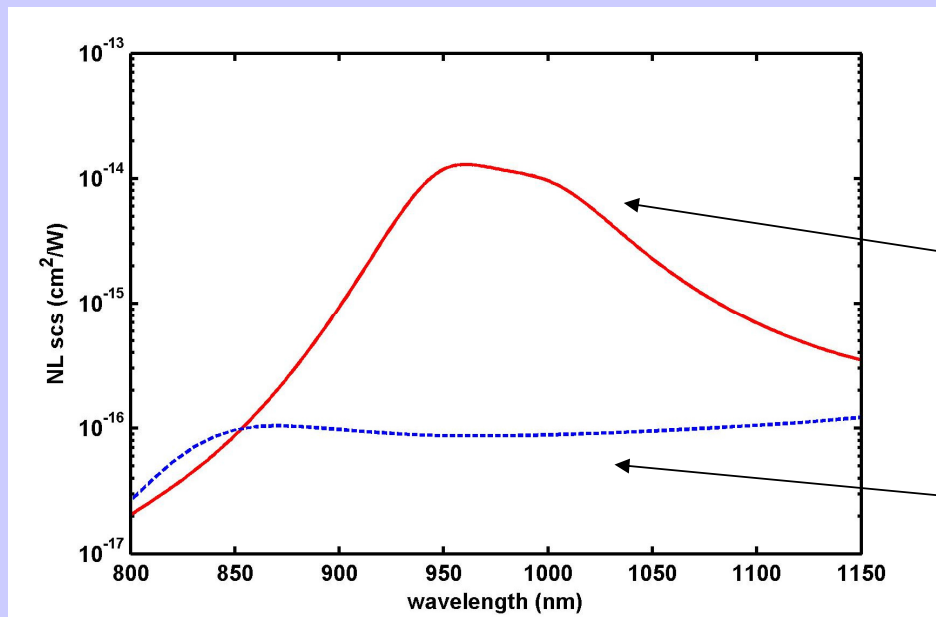
Efficiency factor for absorption at the FF field:

$$Q_{abs} = -\frac{2}{P_{in}} \operatorname{Re} \int_S (\vec{E} \times \vec{H}^*) \cdot \hat{n} dS = -\frac{2R}{I_{in}d} \operatorname{Re} \int_0^{2\pi} (\vec{E} \times \vec{H}^*)_{\hat{n}} d\theta;$$



Silver Coupled Resonators

Enhanced second harmonic non linear scattering cross section due to resonant excitation of a localized surface plasmon polariton in the nanoresonator.



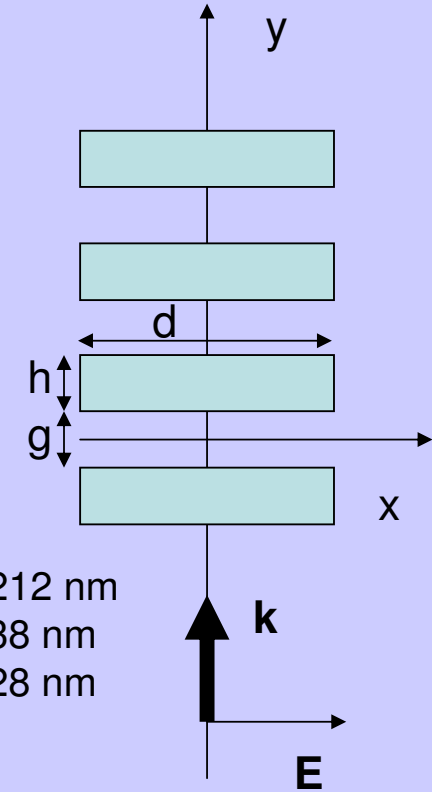
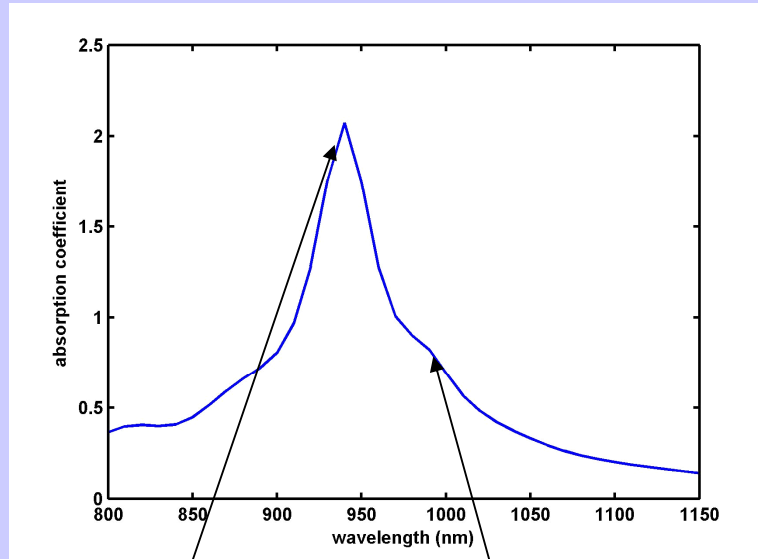
Two-rod nanoresonator

Single rod

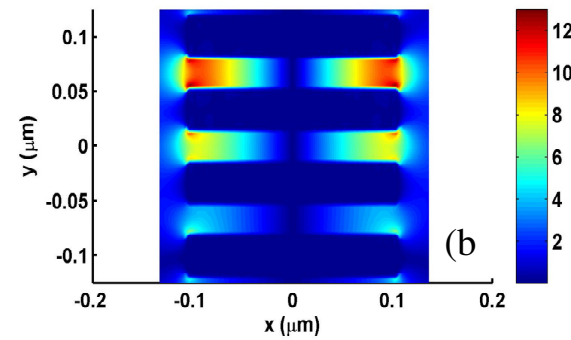
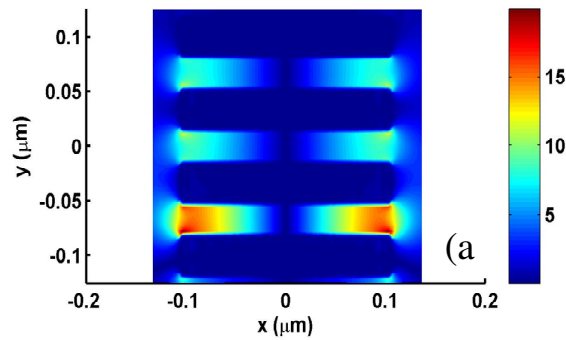
Centini M.; Benedetti A.; Sibilìa C.; Bertolotti M. Coupled 2D Ag nano-resonator chains for enhanced and spatially tailored second harmonic generation OPTICS EXPRESS (2011). 19, 8218- 8232

Silver Coupled Resonators

FF

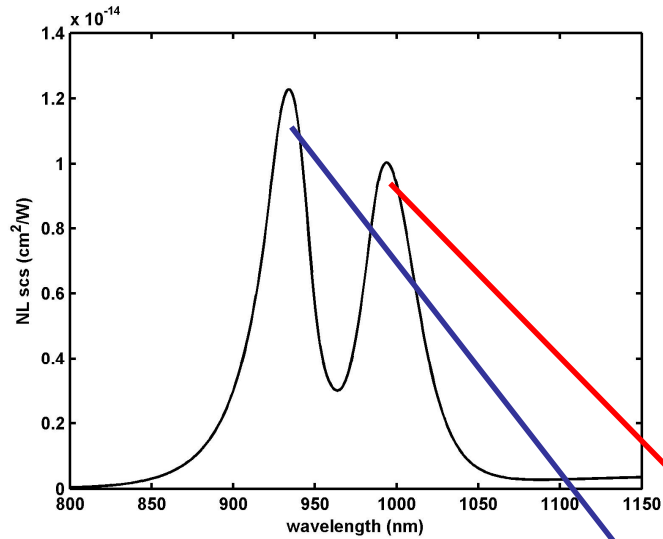


$d=212$ nm
 $h=38$ nm
 $g=28$ nm

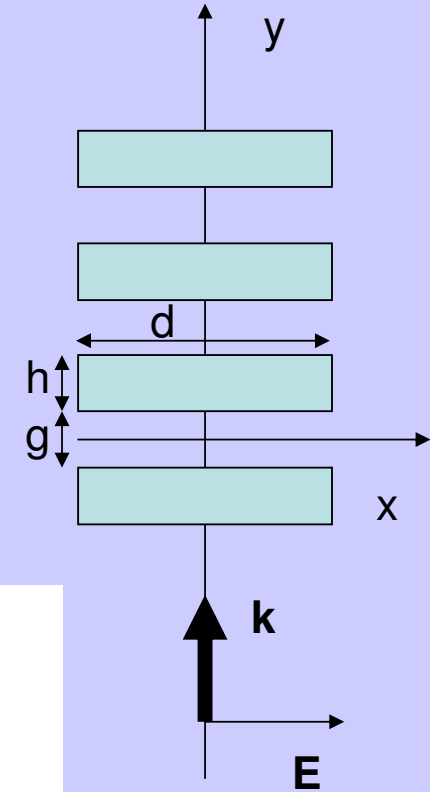
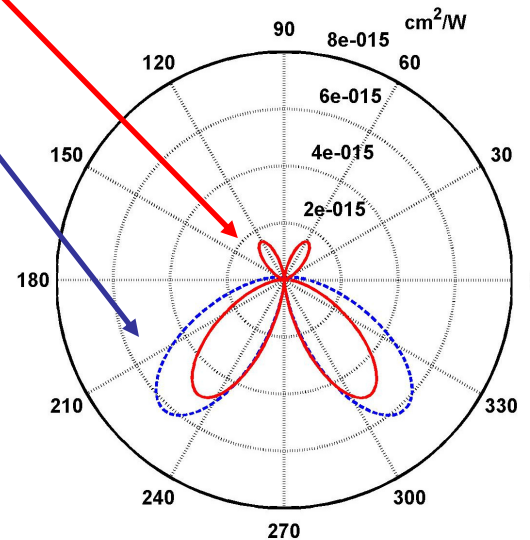


Silver Coupled Resonators

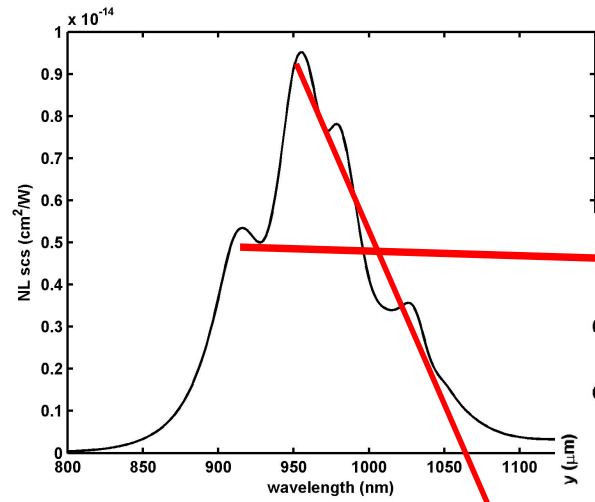
SH



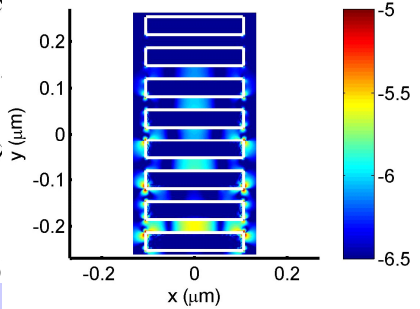
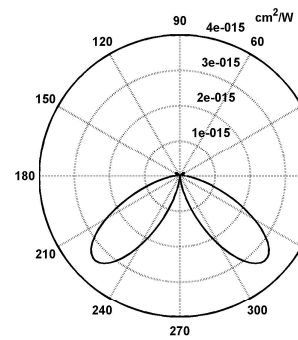
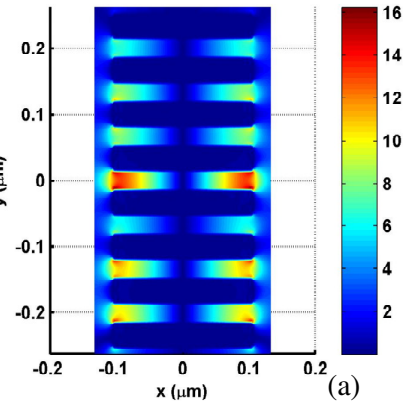
SH far field pattern contains information of the FF sub-wavelength localization properties: Different FF nearfield profiles produce different SH emission patterns.



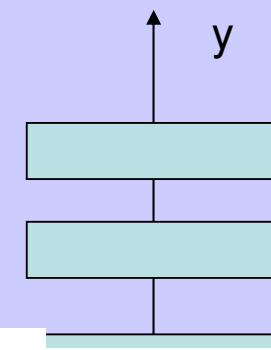
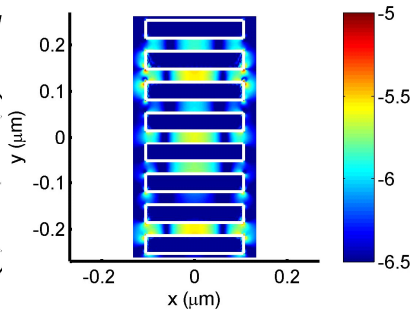
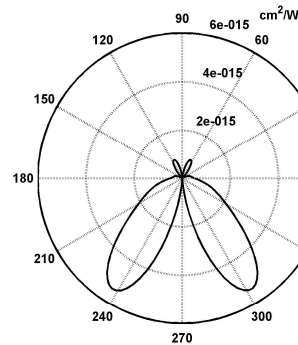
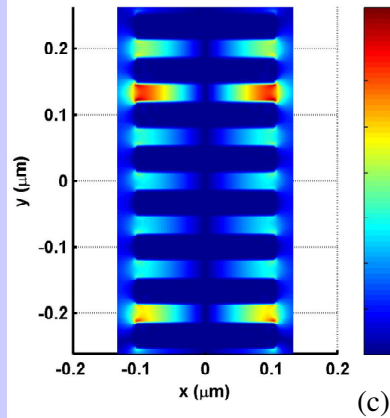
Silver Coupled Resonators



FF @ 920 nm



FF @ 960 nm

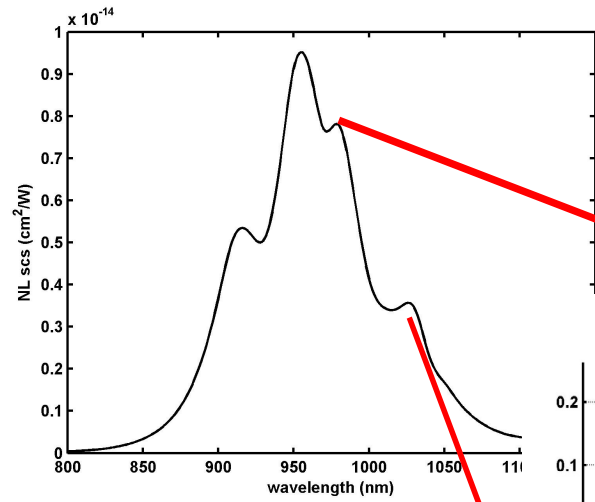


(b)

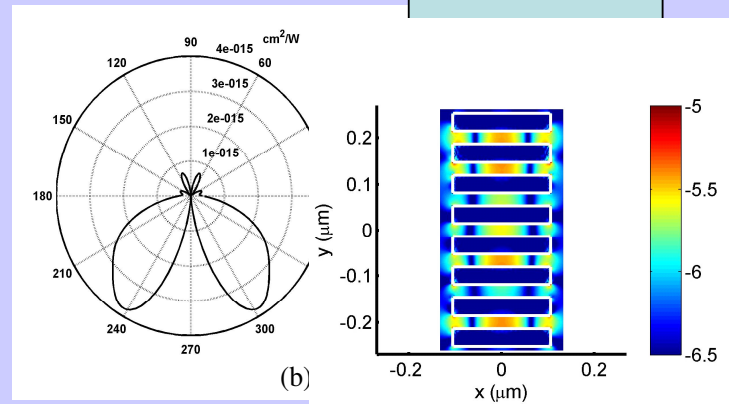
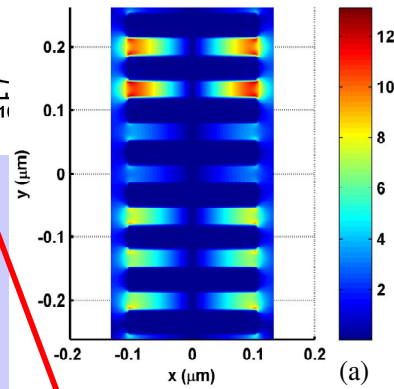
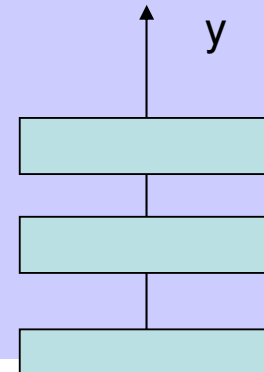
(d)

E

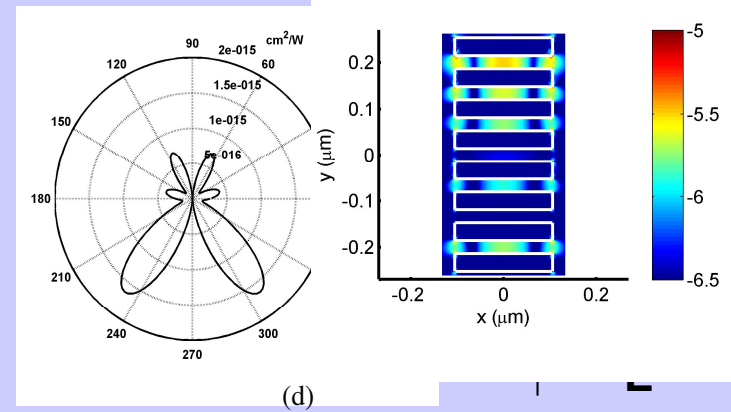
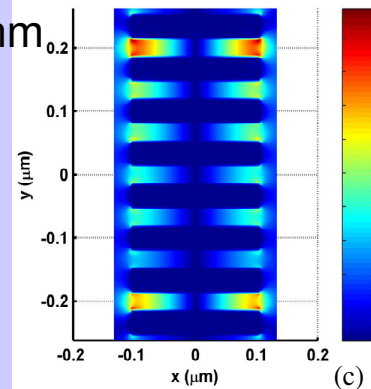
Silver Coupled Resonators



FF @ 980 nm



FF @ 1030 nm



CONCLUSIONS

If nanoantenna's nonlinear response is affected by the excitation of LSPP a variety of cases can be obtained: **great attention must be paid when neglecting the nonlinear surface sources in numerical models of SHG**, because, every case must be considered by itself, without performing a priori simplification.

Different spatial patterns of emission can be achieved by considering surface and/or bulk contributions. Performing experiments with different polarization of the pump field, the two regimes could be addressed in order to investigate dominant surface contributions and dominant bulk contributions separately.

Second harmonic emission pattern of nanostructured arrays of metallic particles can be tailored by changing shapes and distance of the elements.

Considering coupled nanoresonators, near field and far field properties of the generated second harmonic are strictly related to localization properties of the pump field. **The main angle of emission changes as a function of the pump frequency.**

Acknowledgements

Colleagues and collaborators in Rome:

Prof. Mario Bertolotti

Prof. Concita Sibilìa

Dr. Alessio Benedetti

Dr. Mariacristina Larciprete

Dr. Alessandro Belardini